

# *Distortion Varieties*

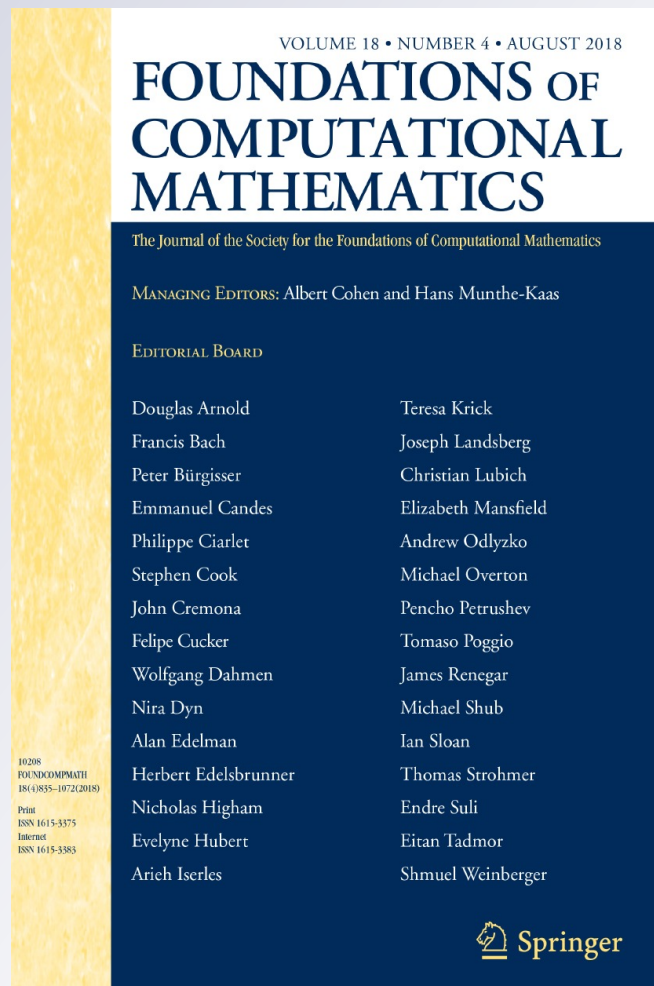
## Joe Kileel, Zuzana Kukelova, Tomas Pajdla & Bernd Sturmfels

### **Foundations of Computational Mathematics**

The Journal of the Society for the Foundations of Computational Mathematics

ISSN 1615-3375  
Volume 18  
Number 4

Found Comput Math (2018)  
18:1043-1071  
DOI 10.1007/s10208-017-9361-0



**Your article is protected by copyright and all rights are held exclusively by SFoCM. This e-offprint is for personal use only and shall not be self-archived in electronic repositories. If you wish to self-archive your article, please use the accepted manuscript version for posting on your own website. You may further deposit the accepted manuscript version in any repository, provided it is only made publicly available 12 months after official publication or later and provided acknowledgement is given to the original source of publication and a link is inserted to the published article on Springer's website. The link must be accompanied by the following text: "The final publication is available at [link.springer.com](http://link.springer.com)".**



## Distortion Varieties

Joe Kileel<sup>1</sup> · Zuzana Kukelova<sup>2</sup> · Tomas Pajdla<sup>3</sup> ·  
Bernd Sturmfels<sup>1</sup>

Received: 10 July 2016 / Revised: 7 October 2016 / Accepted: 6 May 2017 /  
Published online: 7 July 2017  
© SFoCM 2017

**Abstract** The distortion varieties of a given projective variety are parametrized by duplicating coordinates and multiplying them with monomials. We study their degrees and defining equations. Exact formulas are obtained for the case of one-parameter distortions. These are based on Chow polytopes and Gröbner bases. Multi-parameter distortions are studied using tropical geometry. The motivation for distortion varieties comes from multi-view geometry in computer vision. Our theory furnishes a new framework for formulating and solving minimal problems for camera models with image distortion.

**Keywords** Distortion varieties · Toric varieties · Image distortion · Minimal problems

---

Communicated by Joseph M. Landsberg.

---

✉ Joe Kileel  
jkileel@berkeley.edu  
Zuzana Kukelova  
kukelova@cmp.felk.cvut.cz  
Tomas Pajdla  
pajdla@cvut.cz  
Bernd Sturmfels  
bernd@berkeley.edu

- <sup>1</sup> Department of Mathematics, University of California, Berkeley, CA, USA
- <sup>2</sup> Department of Cybernetics, Faculty of Electrical Engineering, Czech Technical University in Prague, Prague, Czech Republic
- <sup>3</sup> Czech Institute of Informatics, Robotics and Cybernetics, Czech Technical University in Prague, Prague, Czech Republic

**Mathematics Subject Classification** 14Q15 · 13P15 · 68T45 · 14M25 · 13P25 · 14T05 · 68U10

## 1 Introduction

This article introduces a construction in algebraic geometry that is motivated by multi-view geometry in computer vision. In that field, one thinks of a camera as a linear projection  $\mathbb{P}^3 \dashrightarrow \mathbb{P}^2$ , and a model is a projective variety  $X \subset \mathbb{P}^n$  that represents the relative positions of two or more such cameras. The data are correspondences of image points in  $\mathbb{P}^2$ . These define a linear subspace  $L \subset \mathbb{P}^n$ , and the task is to compute the real points in the intersection  $L \cap X$  as fast and accurately as possible. See [20, Chapter 9] for a textbook introduction.

A model for cameras with image distortion allows for an additional unknown parameter  $\lambda$ . Each coordinate of  $X$  gets multiplied by a polynomial in  $\lambda$  whose coefficients also depend on the data. We seek to estimate both  $\lambda$  and the point in  $X$ , where the data now specify a subspace  $L'$  in a larger projective space  $\mathbb{P}^N$ . The distortion variety  $X'$  lives in that  $\mathbb{P}^N$ , it satisfies  $\dim(X') = \dim(X) + 1$ , and the task is to compute  $L' \cap X'$  in  $\mathbb{P}^N$  fast and accurately.

We illustrate the idea of distortion varieties for the basic scenario in two-view geometry.

*Example 1.1* The relative position of two uncalibrated cameras is expressed by a  $3 \times 3$ -matrix  $x = (x_{ij})$  of rank 2, known as the *fundamental matrix*. Let  $n = 8$  and write  $\mathcal{F}$  for the hypersurface in  $\mathbb{P}^8$  defined by the  $3 \times 3$ -determinant. Seven (generic) image correspondences in two views determine a line  $L$  in  $\mathbb{P}^8$ , and one rapidly computes the three points in  $L \cap \mathcal{F}$ .

The *8-point radial distortion problem* [25, Section 7.1.3] is modeled as follows in our setting. We introduce six new coordinates  $y_{13}, y_{23}, y_{33}, y_{31}, y_{32}, z_{33}$ . These serve as duplicates for the last row and last column of the  $3 \times 3$ -matrix  $x$ . The resulting  $9 + 6$  unknowns are coordinates on  $\mathbb{P}^{14}$ . We define a rational normal scroll in  $\mathbb{P}^{14}$  by the following parameterization:

$$\begin{aligned} (x_{11} : x_{12} : x_{13} : y_{13} : x_{21} : x_{22} : x_{23} : y_{23} : x_{31} : y_{31} : x_{32} : y_{32} : x_{33} : y_{33} : z_{33}) = \\ (x_{11} : x_{12} : x_{13} : x_{13}\lambda : x_{21} : x_{22} : x_{23} : x_{23}\lambda : x_{31} : x_{31}\lambda : x_{32} : x_{32}\lambda : x_{33} : x_{33}\lambda : x_{33}\lambda^2). \end{aligned} \tag{1}$$

Here  $N = 14$ . The distortion variety  $\mathcal{F}'$  is the closure of the set of points (1) where  $x \in \mathcal{F}$  and  $\lambda \in \mathbb{C}$ . The variety  $\mathcal{F}'$  has dimension 8 and degree 16 in  $\mathbb{P}^{14}$ , whereas  $\mathcal{F}$  has dimension 7 and degree 3 in  $\mathbb{P}^8$ . To estimate both  $\lambda$  and the relative camera positions, we now need eight image correspondences. These data specify a linear space  $L'$  of dimension 6 in  $\mathbb{P}^{14}$ . The task in the computer vision application is to rapidly compute the 16 points in  $L' \cap \mathcal{F}'$ .

The prime ideal of the distortion variety  $\mathcal{F}'$  is minimally generated by 18 polynomials in the 15 variables. First, there are 15 quadratic binomials, namely the  $2 \times 2$ -minors of matrix

$$\begin{pmatrix} x_{13} & x_{23} & x_{31} & x_{32} & x_{33} & y_{33} \\ y_{13} & y_{23} & y_{31} & y_{32} & y_{33} & z_{33} \end{pmatrix}. \tag{2}$$

Note that this matrix has rank 1 under the substitution (1). Second, there are three cubics

$$\begin{aligned}
 &x_{11}x_{22}x_{33} - x_{11}x_{23}x_{32} - x_{12}x_{21}x_{33} + x_{12}x_{23}x_{31} + x_{13}x_{21}x_{32} - x_{13}x_{22}x_{31}, \\
 &x_{13}x_{22}y_{31} - x_{12}x_{23}y_{31} - x_{13}x_{21}y_{32} + x_{11}x_{23}y_{32} + x_{12}x_{21}y_{33} - x_{11}x_{22}y_{33}, \\
 &x_{22}y_{13}y_{31} - x_{12}y_{23}y_{31} - x_{21}y_{13}y_{32} + x_{11}y_{23}y_{32} + x_{12}x_{21}z_{33} - x_{11}x_{22}z_{33}.
 \end{aligned} \tag{3}$$

These three  $3 \times 3$ -determinants replicate the equation that defines the original model  $\mathcal{F}$ .

This paper is organized as follows. Section 2 introduces the relevant concepts and definitions from computer vision and algebraic geometry. We present camera models with image distortion, with focus on distortions with respect to a single-parameter  $\lambda$ . The resulting distortion varieties  $X_{[u]}$  live in the rational normal scroll  $\mathcal{S}_u$ , where  $u = (u_0, u_1, \dots, u_n)$  is a vector of nonnegative integers. This *distortion vector* indicates that the coordinate  $x_i$  on  $\mathbb{P}^n$  is replicated  $u_i$  times when passing to  $\mathbb{P}^N$ . In Example 1.1, we have  $u = (0, 0, 1, 0, 0, 1, 1, 1, 2)$  and  $\mathcal{S}_u$  is the 9-dimensional rational normal scroll defined by the  $2 \times 2$ -minors of (2).

Our results on one-parameter distortions of arbitrary varieties are stated and proved in Sect. 3. Theorem 3.2 expresses the degree of  $X_{[u]}$  in terms of the Chow polytope of  $X$ . Theorem 3.10 derives ideal generators for  $X_{[u]}$  from a Gröbner basis of  $X$ . These results explain what we observed in Example 1.1, namely the degree 16 and the equations in (2)–(3).

Section 4 deals with multi-parameter distortions. We first derive various camera models that are useful for applications, and we then present the relevant algebraic geometry.

Section 5 is concerned with a concrete application to solving minimal problems in computer vision. We focus on the distortion variety  $f + E + \lambda$  of degree 23 derived in Sect. 2.

## 2 One-Parameter Distortions

This section has three parts. First, we derive the relevant camera models from computer vision. Second, we introduce the distortion varieties  $X_{[u]}$  of an arbitrary projective variety  $X$ . And, third, we study the distortion varieties for the camera models from the first part.

### 2.1 Multi-view Geometry with Image Distortion

A *perspective camera* in computer vision [20, page 158] is a linear projection  $\mathbb{P}^3 \dashrightarrow \mathbb{P}^2$ . The  $3 \times 4$ -matrix that represents this map is written as  $K (R | t)$  where  $R \in \text{SO}(3)$ ,  $t \in \mathbb{R}^3$ , and  $K$  is an upper-triangular  $3 \times 3$  matrix known as the calibration matrix. This transforms a point  $Y \in \mathbb{P}^3$  from the world Cartesian coordinate system to the camera Cartesian coordinate system. Here, we usually normalize homogeneous coordinates on  $\mathbb{P}^3$  and  $\mathbb{P}^2$  so that the last coordinate equals 1. With this, points in  $\mathbb{R}^3$  map to  $\mathbb{R}^2$  under the action of the camera.

The following camera model was introduced in [28, Equation 3] to deal with image distortions:

$$\alpha (R | t) Y = \begin{pmatrix} h(\|AU + b\|) (AU + b) \\ g(\|AU + b\|) \end{pmatrix} \quad \text{for some } \alpha \in \mathbb{R} \setminus \{0\}. \quad (4)$$

The two functions  $h: \mathbb{R} \rightarrow \mathbb{R}$  and  $g: \mathbb{R} \rightarrow \mathbb{R}$  represent the distortion. The invertible matrix  $A \in \mathbb{R}^{2 \times 2}$  and the vector  $b \in \mathbb{R}^2$  are used to transform the image point  $U \in \mathbb{R}^2$  into the image Cartesian coordinate system. The perspective camera in the previous paragraph is obtained by setting  $h = g = 1$  and taking the calibration matrix  $K$  to be the inverse of  $\begin{pmatrix} A & b \\ 0 & 1 \end{pmatrix}$ .

Micusik and Pajdla [28] studied applications to fish eye lenses as well as catadioptric cameras. In this context, they found that it often suffices to fix  $h = 1$  and to take a quadratic polynomial for  $g$ . For the following derivation, we choose  $g(t) = 1 + \mu t^2$ , where  $\mu$  is an unknown parameter. We also assume that the calibration matrix has the diagonal form  $K = \text{diag}[f, f, 1]$ . If we set  $\lambda = \mu/f^2$  then the model (4) simplifies to

$$\alpha (R | t) Y = K^{-1} \begin{pmatrix} U \\ 1 + \lambda \|U\|^2 \end{pmatrix} \quad \text{for some } \alpha \in \mathbb{R} \setminus \{0\}. \quad (5)$$

Let us now analyze two-view geometry for the model (5). The quantity  $\lambda = \mu/f^2$  is our distortion parameter. Throughout the discussion in Sect. 2, there is only one such parameter. Later, in Sect. 4, there will be two or more different distortion parameters.

Following [20, Section 9.6], we represent two camera matrices  $(R_1 | t_1)$  and  $(R_2 | t_2)$  by their *essential matrix*  $E$ . This  $3 \times 3$ -matrix has rank 2 and satisfies the *Démazure equations*. The equations were first derived in [10]; they take the matrix form  $2 E E^T E - \text{trace}(E E^T) E = 0$ . For a pair  $(U_1, U_2)$  of corresponding points in two images, the *epipolar constraint* now reads

$$0 = \begin{pmatrix} AU_2 \\ 1 + \mu \|AU_2\|^2 \end{pmatrix}^T E \begin{pmatrix} AU_1 \\ 1 + \mu \|AU_1\|^2 \end{pmatrix} = \begin{pmatrix} U_2 \\ 1 + \lambda \|U_2\|^2 \end{pmatrix}^T K^{-T} E K^{-1} \begin{pmatrix} U_1 \\ 1 + \lambda \|U_1\|^2 \end{pmatrix}. \quad (6)$$

In this way, the essential matrix  $E$  expresses a necessary condition for two points  $U_1$  and  $U_2$  in the image planes to be pictures of the same world point. The *fundamental matrix* is obtained from the essential matrix and the calibration matrix:

$$F = \begin{pmatrix} f_{11} & f_{12} & f_{13} \\ f_{21} & f_{22} & f_{23} \\ f_{31} & f_{32} & f_{33} \end{pmatrix} = K^{-T} E K^{-1}. \quad (7)$$

Using the coordinates of  $U_1 = [u_1, v_1]^T$  and  $U_2 = [u_2, v_2]^T$ , the epipolar constraint (6) is

$$\begin{aligned}
 0 = & u_2 u_1 f_{11} + u_2 v_1 f_{12} + u_2 f_{13} + u_2 \|U_1\|^2 \lambda f_{13} + v_2 u_1 f_{21} + v_2 v_1 f_{22} + v_2 f_{23} \\
 & + v_2 \|U_1\|^2 \lambda f_{23} + u_1 f_{31} + u_1 \|U_2\|^2 \lambda f_{31} + v_1 f_{32} + v_1 \|U_2\|^2 \lambda f_{32} + f_{33} \\
 & + (\|U_1\|^2 + \|U_2\|^2) \lambda f_{33} + \|U_1\|^2 \|U_2\|^2 \lambda^2 f_{33}.
 \end{aligned}$$

This is a sum of 15 terms. The corresponding monomials in the unknowns form the vector

$$m^\top = [f_{11}, f_{12}, f_{13}, f_{13}\lambda, f_{21}, f_{22}, f_{23}, f_{23}\lambda, f_{31}, f_{31}\lambda, f_{32}, f_{32}\lambda, f_{33}, f_{33}\lambda, f_{33}\lambda^2]. \tag{8}$$

The 15 coefficients are real numbers given by the data. The coefficient vector  $c$  is equal to

$$\begin{aligned}
 & [u_2 u_1, u_2 v_1, u_2, u_2 \|U_1\|^2, v_2 u_1, v_2 v_1, v_2, v_2 \|U_1\|^2, u_1, u_1 \|U_2\|^2, v_1, v_1 \\
 & \|U_2\|^2, 1, \|U_1\|^2 + \|U_2\|^2, \|U_1\|^2 \|U_2\|^2]^\top
 \end{aligned}$$

With this notation, the epipolar constraint given by one point correspondence is simply

$$c^\top m = 0. \tag{9}$$

At this stage, we have derived the distortion variety in Example 1.1. Identifying  $f_{ij}$  with the variables  $x_{ij}$ , the vector (8) is precisely the same as that in (1). This is the parametrization of the rational normal scroll  $\mathcal{S}_u$  in  $\mathbb{P}^{14}$  where  $u = (0, 0, 1, 0, 0, 1, 1, 1, 2)$ . The set of fundamental matrices is dense in the hypersurface  $X = \{\det(F) = 0\}$  in  $\mathbb{P}^8$ . Its distortion variety  $X_{[u]}$  has dimension 8 and degree 16 in  $\mathbb{P}^{14}$ . Each point correspondence  $(U_1, U_2)$  determines a vector  $c$ , and hence, a hyperplane in  $\mathbb{P}^{14}$ . The constraint (9) means intersecting  $X_{[u]}$  with that hyperplane. Eight point correspondences determine a 6-dimensional linear space in  $\mathbb{P}^{14}$ . Intersecting  $X_{[u]}$  with that linear subspace is the same as solving the 8-point radial distortion problem in [25, Section 7.1.3]. The expected number of complex solutions is 16.

### 2.2 Scrolls and Distortions

This subsection introduces the algebro-geometric objects studied in this paper. We fix a nonzero vector  $u = (u_0, u_1, \dots, u_n) \in \mathbb{N}^{n+1}$  of nonnegative integers, we abbreviate  $|u| = u_0 + u_1 + \dots + u_n$ , and we set  $N = |u| + n$ . The rational normal scroll  $\mathcal{S}_u$  is a projective variety of dimension  $n + 1$  and degree  $|u|$  in  $\mathbb{P}^N$ . If all  $u_i$  are strictly positive then  $\mathcal{S}_u$  is smooth. The (rational normal) scroll  $\mathcal{S}_u$  has the parametric representation

$$(x_0 : x_0 \lambda : x_0 \lambda^2 : \dots : x_0 \lambda^{u_0} : x_1 : x_1 \lambda : x_1 \lambda^2 : \dots : x_1 \lambda^{u_1} : \dots : x_n : x_n \lambda : \dots : x_n \lambda^{u_n}). \tag{10}$$

The coordinates are monomials, so the scroll  $\mathcal{S}_u$  is also a toric variety [8]. Since  $\text{degree}(\mathcal{S}_u) = |u|$  equals  $\text{codim}(\mathcal{S}_u) + 1 = N - n + 1$ , it is a variety of minimal degree [19, Example 1.14].

Restriction to the coordinates  $(x_0 : x_1 : \dots : x_n)$  defines a rational map  $S_u \dashrightarrow \mathbb{P}^n$ . This is a toric fibration [11]. Its general fibers are curves parametrized by  $\lambda$ . The base locus is a coordinate subspace  $\mathbb{P}^n \subset \mathbb{P}^N$ . Its points are supported on the respectively last coordinates in each of the  $n + 1$  groups. For instance, in Example 2.1 the base locus is the projective plane  $\mathbb{P}^2$  inside  $\mathbb{P}^8$  that is defined by the ideal  $\langle a_0, b_0, b_1, c_0, c_1, c_2 \rangle$ .

The prime ideal of the scroll  $S_u$  is generated by the  $2 \times 2$ -minors of a  $2 \times |u|$ -matrix of unknowns that is obtained by concatenating Hankel matrices on the blocks of unknowns; see [12, Lemma 2.1], [31], and Example 2.1 below. For a textbook reference see [19, Theorem 19.9].

We now consider an arbitrary projective variety  $X$  of dimension  $d$  in  $\mathbb{P}^n$ . This is the underlying model in some application, such as computer vision. We define the *distortion variety of level  $u$* , denoted  $X_{[u]}$ , to be the closure of the preimage of  $X$  under the map  $S_u \dashrightarrow \mathbb{P}^n$ . The general fibers of this map are curves. The distortion variety  $X_{[u]}$  lives in  $\mathbb{P}^N$ . It has dimension  $d + 1$ . Points on  $X_{[u]}$  represent points on  $X$  whose coordinates have been distorted by an unknown parameter  $\lambda$ . Our parameterization is the rule for the distortion. In other words,  $X_{[u]}$  is the closure of the image of the regular map  $X \times \mathbb{C} \rightarrow \mathbb{P}^N$  given by (10).

Each distortion variety represents a *minimal problem* [25] in polynomial systems solving. Data points define linear constraints on  $\mathbb{P}^N$ , like (9). Our problem is to solve  $d + 1$  such linear equations on  $X_{[u]}$ . The number of complex solutions is the degree of  $X_{[u]}$ . A simple bound for that degree is stated in Proposition 3.1, and an exact formula can be found in Theorem 3.2. Of course, in applications we are primarily interested in the real solutions.

We already saw one example of a distortion variety in Example 1.1. In the following example, we discuss some surfaces in  $\mathbb{P}^N$  that arise as distortion varieties of plane curves.

*Example 2.1* Let  $n = 2$  and  $u = (1, 2, 3)$ . The rational normal scroll is a 3-dimensional smooth toric variety in  $\mathbb{P}^8$ . Its implicit equations are the  $2 \times 2$ -minors of the  $2 \times 6$ -matrix

$$\begin{pmatrix} a_0 & b_0 & b_1 & c_0 & c_1 & c_2 \\ a_1 & b_1 & b_2 & c_1 & c_2 & c_3 \end{pmatrix}. \tag{11}$$

This is the “concatenated Hankel matrix” mentioned above. Its pattern generalizes to all distortion vectors  $u$ .

Let  $X$  be a general curve of degree  $d$  in  $\mathbb{P}^2$ . The distortion variety  $X_{[u]}$  is a surface of degree  $5d$  in  $\mathbb{P}^8$ . Its prime ideal is generated by the 15 minors of (11) together with  $d + 1$  polynomials of degree  $d$ . These are obtained from the ternary form that defines  $X$  by the distortion process in Theorem 3.10. For special curves  $X$ , the degree of  $X_{[u]}$  may drop below  $5d$ . For instance, given a line  $X = V(\lambda a + \mu b + \nu c)$  in  $\mathbb{P}^2$ , the distortion surface  $X_{[u]}$  has degree 5 if  $\lambda \neq 0$ , it has degree 4 if  $\lambda = 0$  but  $\mu \neq 0$ , and it has degree 3 if  $\lambda = \mu = 0$ . For any curve  $X$ , the property  $\deg(X_{[u]}) = 5 \cdot \deg(X)$  holds after a coordinate change in  $\mathbb{P}^2$ . If  $X = \{p\}$  is a single point in  $\mathbb{P}^2$  then  $X_{[u]}$  is a curve in  $\mathbb{P}^8$ . It has degree 3 unless  $p \in V(c)$ .

### 2.3 Back to Two-View Geometry

In this subsection, we describe several variants of Example 1.1. These highlight the role of distortion varieties in two-view geometry. We fix  $n = 8$ ,  $N = 14$  and  $u = (0, 0, 1, 0, 0, 1, 1, 1, 2)$  as above. The scroll  $\mathcal{S}_u$  is the image of the map (1) and its ideal is generated by the  $2 \times 2$ -minors of (2). Each of the following varieties live in the space of  $3 \times 3$ -matrices  $x = (x_{ij})$ .

*Example 2.2* (Essential matrices) We now write  $\mathcal{E}$  for the essential variety [10, 16]. It has dimension 5 and degree 10 in  $\mathbb{P}^8$ . Its real points  $x$  are the essential matrices in (6). The ideal of  $\mathcal{E}$  is generated by ten cubics, namely  $\det(x)$  and the nine entries of the matrix  $2xx^T x - \text{trace}(xx^T)x$ . The distortion variety  $\mathcal{E}_{[u]}$  has dimension 6 and degree 52 in  $\mathbb{P}^{14}$ . Its ideal is generated by 15 quadrics and 18 cubics, derived from the ten D emazure cubics.

*Example 2.3* (Essential matrices plus two equal focal lengths) Fix a diagonal calibration matrix  $k = \text{diag}(f, f, 1)$ , where  $f$  is a new unknown. We define  $\mathcal{G}$  to be the closure in  $\mathbb{P}^8$  of the set of  $3 \times 3$ -matrices  $x$  such that  $kxk \in \mathcal{E}$  for some  $f$ . To compute the ideal of the variety  $\mathcal{G}$ , we use the following lines of code in the computer algebra system Macaulay2 [18]:

```
R = QQ[f, x11, x12, x13, x21, x22, x23, x31, x32, x33, y13, y23,
      y33, y31, y32, z33, t];
X = matrix {{x11, x12, x13}, {x21, x22, x23}, {x31, x32, x33}}
K = matrix {{f, 0, 0}, {0, f, 0}, {0, 0, 1}};
P = K*X*K;
E = minors(1, 2*P*transpose(P)*P-trace(P*transpose(P))*P)
    +ideal(det(P));
G = eliminate({f}, saturate(E, ideal(f)))
codim G, degree G, betti mingens G
```

The output tells us that the variety  $\mathcal{G}$  has dimension 6 and degree 15 and that  $\mathcal{G}$  is the complete intersection of two hypersurfaces in  $\mathbb{P}^8$ , namely the cubic  $\det(x)$  and the quintic

$$\begin{aligned}
 &x_{11}x_{13}^3x_{31} + x_{13}^2x_{21}x_{23}x_{31} + x_{11}x_{13}x_{23}^2x_{31} + x_{21}x_{23}^3x_{31} - x_{11}x_{13}x_{31}^3 - x_{21}x_{23}x_{31}^3 \\
 &\quad + x_{12}x_{13}^3x_{32} + x_{13}^2x_{22}x_{23}x_{32} + x_{12}x_{13}x_{23}^2x_{32} + x_{22}x_{23}^3x_{32} - x_{12}x_{13}x_{31}^2x_{32} \\
 &\quad - x_{12}^2x_{13}^2x_{33} - x_{11}x_{13}x_{31}x_{32}^2 - x_{21}x_{23}x_{31}x_{32}^2 - x_{12}x_{13}x_{32}^3 - x_{22}x_{23}x_{32}^3 \\
 &\quad - x_{11}^2x_{13}^2x_{33} - x_{22}x_{23}x_{31}^2x_{32} - 2x_{11}x_{13}x_{21}x_{23}x_{33} - 2x_{12}x_{13}x_{22}x_{23}x_{33} - x_{21}^2x_{23}^2x_{33} \\
 &\quad - x_{22}^2x_{23}^2x_{33} + x_{11}^2x_{31}^2x_{33} + x_{21}^2x_{31}^2x_{33} + 2x_{11}x_{12}x_{31}x_{32}x_{33} \\
 &\quad + 2x_{21}x_{22}x_{31}x_{32}x_{33} + x_{12}^2x_{32}^2x_{33} + x_{22}^2x_{32}^2x_{33}.
 \end{aligned}
 \tag{12}$$

The distortion variety  $\mathcal{G}_{[u]}$  is now computed by the following lines in Macaulay2:

```
Gu = eliminate({t}, G +
  ideal(y13-x13*t, y23-x23*t, y31-x31*t, y32-x32*t, y33-x33*t,
        z33-x33*t^2))
codim Gu, degree Gu, betti mingens Gu
```

**Table 1** Dimensions and degrees of two-view models and their radial distortions

$u = (0, 0, 1, 0, 0, 1, 1, 1, 2)$	Ref.	$n$	$N$	$\dim(X)$	$\deg(X)$	$\dim(X_{[u]})$	$\deg(X_{[u]})$	Proposition 3.1
$\mathcal{F}$ in Example 1.1: $\lambda + F + \lambda$	[25]	8	14	7	3	8	16	18
$\mathcal{E}$ in Example 2.2: $\lambda + E + \lambda$	[25]	8	14	5	10	6	52	60
$\mathcal{G}$ in Example 2.3: $\lambda f + E + f\lambda$	[22]	8	14	6	15	7	68	90
$\mathcal{G}'$ in Example 2.4: $\lambda + E + f\lambda$		8	14	6	9	7	42	54
$v = (0, 0, 1, 0, 0, 1, 0, 0, 1)$	Ref.	$n$	$N$	$\dim(X)$	$\deg(X)$	$\dim(X_{[v]})$	$\deg(X_{[v]})$	Proposition 3.1
$\mathcal{F}$ in Example 2.5: $F + \lambda$	[24]	8	11	7	3	8	8	9
$\mathcal{E}$ in Example 2.5: $E + \lambda$	[24]	8	11	5	10	6	26	30
$\mathcal{G}$ in Example 2.5: $f + E + f\lambda$		8	11	6	15	7	37	45
$\mathcal{G}'$ in Example 2.5: $E + f\lambda$	[24]	8	11	6	9	7	19	27
$\mathcal{G}''$ in Example 2.5: $f + E + \lambda$		8	11	6	9	7	23	27

We learn that  $\mathcal{G}_{[u]}$  has dimension 7 and degree 68 in  $\mathbb{P}^{14}$ . Modulo the 15 quadrics for  $\mathcal{S}_u$ , its ideal is generated by three cubics, like those in (3), and five quintics, derived from (12).

*Example 2.4* (Essential matrices plus one focal length unknown) Let  $\mathcal{G}'$  denote the 6-dimensional subvariety of  $\mathbb{P}^8$  defined by the four maximal minors of the  $3 \times 4$ -matrix

$$\begin{pmatrix} x_{11} & x_{12} & x_{13} & x_{21}x_{31} + x_{22}x_{32} + x_{23}x_{33} \\ x_{21} & x_{22} & x_{23} & -x_{11}x_{31} - x_{12}x_{32} - x_{13}x_{33} \\ x_{31} & x_{32} & x_{33} & 0 \end{pmatrix}. \tag{13}$$

This variety has dimension 6 and degree 9 in  $\mathbb{P}^8$ . It is defined by one cubic and three quartics. The variety  $\mathcal{G}'$  is similar to  $\mathcal{G}$  in Example 2.3, but with the identity matrix as the calibration matrix for one of the two cameras. We can compute  $\mathcal{G}'$  by running the Macaulay2 code above but with the line  $\mathbb{P} = \mathbb{K} * X * \mathbb{K}$  replaced with the line  $\mathbb{P} = X * \mathbb{K}$ . This model was studied in [4].

The distortion variety  $\mathcal{G}'_{[u]}$  has dimension 7 and degree 42 in  $\mathbb{P}^{14}$ . Modulo the 15 quadrics that define  $\mathcal{S}_u$ , the ideal of  $\mathcal{G}'_{[u]}$  is minimally generated by three cubics and 11 quartics.

Table 1 summarizes the four models we discussed in Examples 1.1, 2.2, 2.3 and 2.4. The first column points to a reference in computer vision where this model has been studied. The last column shows the upper bound for  $\deg(X_{[u]})$  given in Proposition 3.1. That bound is not tight in any of our examples. In the second half of the table, we report the same data for the four models when only one of the two cameras undergoes radial distortion.

*Example 2.5* We revisit the four two-view models discussed above, but with distortion vector  $v = (0, 0, 1, 0, 0, 1, 0, 0, 1)$ . Now,  $N = 11$  and only one camera is distorted.

The rational normal scroll  $\mathcal{S}_v$  has codimension 2 and degree 3 in  $\mathbb{P}^{11}$ . Its parametric representation is

$$(x_{11} : x_{12} : x_{13} : x_{13}\lambda : x_{21} : x_{22} : x_{23} : x_{23}\lambda : x_{31} : x_{32} : x_{33} : x_{33}\lambda).$$

The distortion varieties  $\mathcal{F}_{[v]}$ ,  $\mathcal{E}_{[v]}$ ,  $\mathcal{G}_{[v]}$  and  $\mathcal{G}'_{[v]}$  live in  $\mathbb{P}^{11}$ . Their degrees are shown in the lower half of Table 1. For instance, consider the last two rows. The notation  $E + f\lambda$  means that the right camera has unknown focal length and it is also distorted.

The fifth row refers to another variety  $\mathcal{G}''$ . This is the image of  $\mathcal{G}'$  under the linear isomorphism that maps a  $3 \times 3$ -matrix to its transpose. Since  $v$  is not a symmetric matrix, unlike  $u$ , the variety  $\mathcal{G}''_{[v]}$  is actually different from  $\mathcal{G}'_{[v]}$ . The descriptor  $f + E + \lambda$  of  $\mathcal{G}''_{[v]}$  expresses that the left camera has unknown focal length and the right camera is distorted. The variety  $\mathcal{G}''_{[v]}$  has dimension 7 and degree 23 in  $\mathbb{P}^{11}$ . In addition to the three quadrics  $x_{3i}y_{3j} - x_{3j}y_{3i}$  that define  $\mathcal{S}_v$ , the ideal generators for  $\mathcal{G}''_{[v]}$  are two cubics and five quartics. The minimal problem for this distortion variety is studied in detail in Sect. 5.

### 3 Equations and Degrees

In this section, we express the degree and equations of  $X_{[u]}$  in terms of those of  $X$ . Throughout we assume that  $X$  is an irreducible variety of codimension  $c$  in  $\mathbb{P}^n$  and the distortion vector  $u \in \mathbb{N}^{n+1}$  satisfies  $u_0 \leq u_1 \leq \dots \leq u_n$ . We begin with a general upper bound for the degree of the distortion variety  $X_{[u]}$ .

**Proposition 3.1** *Suppose  $u_n \geq 1$ . The degree of the distortion variety satisfies*

$$\deg(X_{[u]}) \leq \deg(X) \cdot (u_c + u_{c+1} + \dots + u_n). \tag{14}$$

*This holds with equality if the coordinates are chosen so that  $X$  is in general position in  $\mathbb{P}^n$ .*

The upper bound in Proposition 3.1 is shown for our models in the last column of Table 1. This result will be strengthened in Theorem 3.2 below, where we give an exact degree formula that works for all  $X$ . It is instructive to begin with the two extreme cases. If  $c = 0$  and  $X = \mathbb{P}^n$ , then we recover the fact that the scroll  $X_{[u]} = \mathcal{S}_u$  has degree  $N - n = u_0 + \dots + u_n$ . If  $c = n$  and  $X$  is a general point in  $\mathbb{P}^n$ , then  $X_{[u]}$  is a rational normal curve of degree  $u_n$ .

The following proof, and the subsequent development in this section, assumes familiarity with two tools from computational algebraic geometry: the construction of *initial ideals* with respect to weight vectors, as in [34], and the *Chow form* of a projective variety [9, 16, 17, 23].

*Proof of Proposition 3.1* Fix  $\dim(X_{[u]}) = n - c + 1$  general linear forms on  $\mathbb{P}^N$ , denoted  $\ell_0, \ell_1, \dots, \ell_{n-c}$ . We write their coefficients as the rows of the  $(n - c + 1) \times$

$(N + 1)$  matrix

$$\begin{bmatrix} \alpha_{0,0} & \alpha_{0,1} & \alpha_{0,2} & \cdots & \alpha_{0,N} \\ \alpha_{1,0} & \alpha_{1,1} & \alpha_{1,2} & \cdots & \alpha_{1,N} \\ \vdots & \vdots & \vdots & \ddots & \vdots \\ \alpha_{n-c,0} & \alpha_{n-c,1} & \alpha_{n-c,2} & \cdots & \alpha_{n-c,N} \end{bmatrix}. \tag{15}$$

Here  $\alpha_{i,j} \in \mathbb{C}$ . The degree of  $X_{[u]}$  equals  $\#(X_{[u]} \cap V(\ell_0, \dots, \ell_{n-c}))$ . We shall do this count. Recall that  $X_{[u]}$  is the closure of the image of the injective map  $X \times \mathbb{C} \rightarrow \mathbb{P}^N$  given in (10). The image of this map is dense in  $X_{[u]}$ . Its complement is the  $\mathbb{P}^n$  consisting of all points whose coordinates in each the  $n + 1$  groups are zero except for the last one. Since the linear forms  $\ell_i$  are generic, all points of  $X_{[u]} \cap V(\ell_0, \dots, \ell_{n-c})$  lie in this image. By injectivity of the map,  $\text{deg}(X_{[u]})$  is the number of pairs  $(x, \lambda) \in X \times \mathbb{C}$  which map into  $X_{[u]} \cap V(\ell_0, \dots, \ell_{n-c})$ .

We formulate this condition on  $(x, \lambda)$  as follows. Consider the  $(n - c + 1) \times (n + 1)$  matrix

$$\begin{bmatrix} \alpha_{0,0} + \alpha_{0,1}\lambda + \cdots + \alpha_{0,u_0}\lambda^{u_0} & \cdots & \alpha_{0,u_0+\dots+u_{n-1}+n} + \cdots + \alpha_{0,N}\lambda^{u_n} \\ \alpha_{1,0} + \alpha_{1,1}\lambda + \cdots + \alpha_{1,u_0}\lambda^{u_0} & \cdots & \alpha_{1,u_0+\dots+u_{n-1}+n} + \cdots + \alpha_{1,N}\lambda^{u_n} \\ \vdots & \ddots & \vdots \\ \alpha_{n-c,0} + \alpha_{n-c,1}\lambda + \cdots + \alpha_{n-c,u_0}\lambda^{u_0} & \cdots & \alpha_{n-c,u_0+\dots+u_{n-1}+n} + \cdots + \alpha_{n-c,N}\lambda^{u_n} \end{bmatrix}. \tag{16}$$

We want to count pairs  $(x, \lambda) \in \mathbb{P}^n \times \mathbb{C}$  such that  $x \in X$  and  $x$  lies in the kernel of this matrix. By genericity of  $\ell_i$ , this matrix has rank  $n - c + 1$  for all  $\lambda \in \mathbb{C}$ . This means that, for each  $\lambda \in \mathbb{C}$ , the kernel of the matrix (16) is a linear subspace of dimension  $c - 1$  in  $\mathbb{P}^n$ .

We conclude that (16) defines a rational curve in the Grassmannian  $\text{Gr}(\mathbb{P}^{c-1}, \mathbb{P}^n)$ . Here, the  $\alpha_{i,j}$  are fixed generic complex numbers and  $\lambda$  is an unknown that parametrizes the curve. If we take the Grassmannian in its Plücker embedding, then the degree of our curve is  $u_c + u_{c+1} + \cdots + u_n$ , which is the largest degree in  $\lambda$  of any maximal minor of (16).

At this point, we use the *Chow form*  $\text{Ch}_X$  of the variety  $X$ . Following [9, 17], this is the defining equation of an irreducible hypersurface in the Grassmannian  $\text{Gr}(\mathbb{P}^{c-1}, \mathbb{P}^n)$ . Its points are the subspaces that intersect  $X$ . The degree of  $\text{Ch}_X$  in Plücker coordinates is  $\text{deg}(X)$ .

We now consider the intersection of our curve with the hypersurface defined by  $\text{Ch}_X$ . Equivalently, we substitute the maximal minors of (16) into  $\text{Ch}_X$  and we examine the resulting polynomial in  $\lambda$ . Since the matrix entries  $\alpha_{i,j}$  in (15) are generic, the curve intersects the hypersurface of the Chow form  $\text{Ch}_X$  outside its singular locus. By Bézout's Theorem, the number of intersection points is bounded above by  $\text{deg}(X) \cdot (u_c + u_{c+1} + \cdots + u_n)$ .

Each intersection point is nonsingular on  $V(\text{Ch}_X)$ , and so the corresponding linear space intersects the variety  $X$  in a unique point  $x$ . We conclude that the number of desired pairs  $(x, \lambda)$  is at most  $\text{deg}(X) \cdot (u_c + u_{c+1} + \cdots + u_n)$ . This establishes the upper bound.

For the second assertion, we apply a general linear change of coordinates to  $X$  in  $\mathbb{P}^n$ . Consider the lexicographically last Plücker coordinate, denoted  $p_{c,c+1,\dots,n}$ . The

monomial  $p_{c,c+1,\dots,n}^{\deg(X)}$  appears with nonzero coefficient in the Chow form  $\text{Ch}_X$ . Substituting the maximal minors of (16) into  $\text{Ch}_X$ , we obtain a polynomial in  $\lambda$  of degree  $\deg(X) \cdot (u_c + u_{c+1} + \dots + u_n)$ . By the genericity hypothesis on (15), this polynomial has distinct roots in  $\mathbb{C}$ . These represent distinct points in  $X_{[u]} \cap V(\ell_0, \dots, \ell_{n-c})$ , and we conclude that the upper bound is attained.  $\square$

We will now refine the method in the proof above to derive an exact formula for the degree of  $X_{[u]}$  that works in all cases. The Chow form  $\text{Ch}_X$  is expressed in primal Plücker coordinates  $p_{i_0,i_1,\dots,i_{n-c}}$  on  $\text{Gr}(\mathbb{P}^{c-1}, \mathbb{P}^n)$ . The *weight* of such a coordinate is the vector  $e_{i_0} + e_{i_1} + \dots + e_{i_{n-c}}$ , and the weight of a monomial is the sum of the weights of its variables. The *Chow polytope* of  $X$  is the convex hull of the weights of all Plücker monomials appearing in  $\text{Ch}_X$ ; see [23].

**Theorem 3.2** *The degree of  $X_{[u]}$  is the maximum value attained by the linear functional  $w \mapsto u \cdot w$  on the Chow polytope of  $X$ . This positive integer can be computed by the formula*

$$\text{degree}(X_{[u]}) = \sum_{j=0}^n u_j \cdot \text{degree}(\text{in}_{-u}(X) : \langle x_j \rangle^\infty), \tag{17}$$

where  $\text{in}_{-u}(X)$  is the initial monomial ideal of  $X$  with respect to a term order that refines  $-u$ .

*Proof* Let  $M$  be a monomial ideal in  $x_0, x_1, \dots, x_n$  whose variety is pure of codimension  $c$ . Each of its irreducible components is a coordinate subspace  $\text{span}(e_{i_0}, e_{i_1}, \dots, e_{i_{n-c}})$  of  $\mathbb{P}^n$ . We write  $\mu_{i_0,i_1,\dots,i_{n-c}}$  for the multiplicity of  $M$  along that coordinate subspace. By [23, Theorem 2.6], the Chow form of (the cycle given by)  $M$  is the Plücker monomial  $\prod p_{i_0,i_1,\dots,i_{n-c}}^{\mu_{i_0,i_1,\dots,i_{n-c}}}$ , and the Chow polytope of  $M$  is the point  $\sum \mu_{i_0,i_1,\dots,i_{n-c}}(e_{i_0} + e_{i_1} + \dots + e_{i_{n-c}})$ . The  $j$ -th coordinate of that point can be computed from  $M$  without performing a monomial primary decomposition. Namely, the  $j$ -th coordinate of the Chow point of  $M$  is the degree of the saturation  $M : \langle x_j \rangle^\infty$ . This follows from [23, Proposition 3.2] and the proof of [23, Theorem 3.3].

We now substitute each maximal minor of the matrix (16) for the corresponding Plücker coordinate  $p_{i_0,i_1,\dots,i_{n-c}}$ . This results in a general polynomial of degree  $u_{i_0} + u_{i_1} + \dots + u_{i_{n-c}}$  in the one unknown  $\lambda$ . When carrying out this substitution in the Chow form  $\text{Ch}_X$ , the highest degree terms do not cancel, and we obtain a polynomial in  $\lambda$  whose degree is the largest  $u$ -weight among all Plücker monomials in  $\text{Ch}_X$ . Equivalently, this degree in  $\lambda$  is the maximum inner product of the vector  $u$  with any vertex of the Chow polytope of  $X$ .

One vertex that attains this maximum is the Chow point of the monomial ideal  $M = \text{in}_{-u}(X)$  in the proof of Proposition 3.1. Note that we had chosen one particular term order to refine the partial order given by  $-u$ . If we vary that term order, then we obtain all vertices on the face of the Chow polytope supported by  $u$ . The saturation formula for the Chow point of the monomial ideal  $M$  in the first paragraph of the proof completes our argument.  $\square$

We are now able to characterize when the upper bound in Proposition 3.1 is attained. Let  $c_-$  and  $c_+$  be the smallest and largest index, respectively, such that  $u_{c_-} = u_c = u_{c_+}$ . We define a set  $\mathcal{L}_u$  of  $n - c + 1$  linear forms as follows. Start with the  $n - c_+$  variables  $x_{c_++1}, x_{c_++2}, \dots, x_n$  and then take  $c_+ - c + 1$  generic linear forms in the variables  $x_{c_-}, x_{c_-+1}, \dots, x_{c_+}$ . In the case when  $u$  has distinct coordinates,  $V(\mathcal{L}_u)$  is simply the subspace spanned by  $e_0, e_1, \dots, e_{n-c}$ .

**Corollary 3.3** *The degree of  $X_{[u]}$  is the right hand side of (14) if and only if  $V(\mathcal{L}_u) \cap X = \emptyset$ .*

*Proof* The quantity  $\deg(X) \cdot (u_c + u_{c+1} + \dots + u_n)$  is the maximal  $u$ -weight among Plücker monomials of degree equal to  $\deg(X)$ . The monomials that attain this maximal  $u$ -weight are products of  $\deg(X)$  many Plücker coordinates of weight  $u_c + u_{c+1} + \dots + u_n$ . These are precisely the Plücker coordinates  $p_{i_0, i_1, \dots, i_{c_+-c}, u_{c_++1}, \dots, u_n}$ , where  $c_- \leq i_0 < i_1 < \dots < i_{c_+-c} \leq c_+$ .

Such monomials are nonzero when evaluated at the subspace  $V(\mathcal{L}_u)$ . All other monomials, namely those having smaller  $u$ -weight, evaluate to zero on  $V(\mathcal{L}_u)$ . Hence, the Chow form  $\text{Ch}_X$  has terms of degree  $\deg(X) \cdot (u_c + u_{c+1} + \dots + u_n)$  if and only if  $\text{Ch}_X$  evaluates to a nonzero constant on  $V(\mathcal{L})$  if and only if the intersection of  $X$  with  $V(\mathcal{L}_u)$  is empty. □

We present two examples to illustrate the exact degree formula in Theorem 3.2.

*Example 3.4* Suppose  $X$  is a hypersurface in  $\mathbb{P}^n$ , defined by a homogeneous polynomial  $\psi(x_0, \dots, x_n)$  of degree  $d$ . Let  $\Psi$  be the tropicalization of  $\psi$ , with respect to min-plus algebra, as in [27]. Equivalently,  $\Psi$  is the support function of the Newton polytope of  $f$ . Then

$$\deg(X_{[u]}) = d \cdot |u| - \Psi(u_0, u_1, \dots, u_n). \tag{18}$$

For instance, let  $n = 8, d = 3$  and  $\psi$  the determinant of a  $3 \times 3$ -matrix. Hence,  $X$  is the variety of fundamental matrices, as in Example 1.1. The tropicalization of the  $3 \times 3$ -determinant is

$$\Psi = \min(u_{11}+u_{22}+u_{33}, u_{11}+u_{23}+u_{32}, u_{12}+u_{21}+u_{33}, u_{12}+u_{23}+u_{31}, u_{13}+u_{21}+u_{32}, u_{13}+u_{22}+u_{31}).$$

The degree of the distortion variety  $X_{[u]}$  equals  $3 \cdot \sum u_{ij} - \Psi$ . This explains the degree 16 we had observed in Example 1.1 for the radial distortion of the fundamental matrices.

*Example 3.5* Let  $X$  be the variety of essential matrices with the same distortion vector  $u$ . In Example 2.2, we found that  $\deg(X_{[u]}) = 52$ . The following Macaulay2 code verifies this:

```
U = {0, 0, 1, 0, 0, 1, 1, 1, 2};
R = QQ[x11, x12, x13, x21, x22, x23, x31, x32, x33, Weights
=>apply(U, i->10-i)];
```

```
P = matrix {{x11,x12,x13},{x21,x22,x23},{x31,x32,x33}}
X = minors(1,2*P*transpose(P)*P-trace(P*transpose(P))*P)
  +ideal(det(P));
M = ideal leadTerm X;
sum apply( 9, i -> U_i * degree(saturate(M,ideal
  ((gens R)_i))) )
```

Here,  $M$  is the monomial ideal in  $\mathbb{C}[U_i]$ , and the last line is our saturation formula in (17).

We next derive the equations that define the distortion variety  $X_{[u]}$  from those that define the underlying variety  $X$ . Our point of departure is the ideal of the rational normal scroll  $\mathcal{S}_u$ . It is generated by the  $\binom{N-n}{2}$  minors of the concatenated Hankel matrix. The following lemma is well known and easy to verify using Buchberger’s S-pair criterion; see also [31].

**Lemma 3.6** *The  $2 \times 2$ -minors that define the rational normal scroll  $\mathcal{S}_u$  form a Gröbner basis with respect to the diagonal monomial order. The initial monomial ideal is square-free.*

For instance, in Example 2.1, when  $n = 2$  and  $u = (1, 2, 3)$ , the initial monomial ideal is

$$\langle a_0b_1, a_0b_2, a_0c_1, a_0c_2, a_0c_3, b_0b_2, b_0c_1, b_0c_2, b_0c_3, b_1c_1, b_1c_2, b_1c_3, c_0c_2, c_0c_3, c_1c_3 \rangle. \quad (19)$$

A monomial  $m$  is *standard* if it does not lie in this initial ideal. The *weight* of a monomial  $m$  is the sum of its indices. Equivalently, the weight of  $m$  is the degree in  $\lambda$  of the monomial in  $N + 1$  variables that arises from  $m$  when substituting in the parametrization of  $\mathcal{S}_u$ .

**Lemma 3.7** *Consider any monomial  $x^v = x_0^{v_0}x_1^{v_1} \cdots x_n^{v_n}$  of degree  $|v|$  in the coordinates of  $\mathbb{P}^n$ . For any nonnegative integer  $i \leq v \cdot u$ , there exists a unique monomial  $m$  in the coordinates on  $\mathbb{P}^N$  such that  $m$  is standard and maps to  $x^v\lambda^i$  under the parameterization of the scroll  $\mathcal{S}_u$ .*

*Proof* The polyhedral cone corresponding to the toric variety  $\mathcal{S}_u$  consists of all pairs  $(v, i) \in \mathbb{R}_{\geq 0}^{n+2}$  with  $0 \leq i \leq v \cdot u$ . Its lattice points correspond to monomials  $x^v t^i$  on  $\mathcal{S}_u$ . Since the initial ideal in Lemma 3.6 is square-free, the associated regular triangulation of the polytope is unimodular, by [34, Corollary 8.9]. Each lattice point  $(v, i)$  has a unique representation as an  $\mathbb{N}$ -linear combination of generators that span a cone in the triangulation. Equivalently,  $x^v t^i$  has a unique representation as a standard monomial in the  $N + 1$  coordinates on  $\mathbb{P}^N$ .  $\square$

We refer to the standard monomial  $m$  in Lemma 3.7 as the  $i$ th *distortion* of the given  $x^v$ .

**Example 3.8** In Example 2.1, we have  $n = 2$ ,  $N = 8$ , and  $\mathcal{S}_u$  corresponds to the cone over a triangular prism. The lattice points in that cone are the monomials  $x_0^{v_0}x_1^{v_1}x_2^{v_2}t^i$  with  $0 \leq i \leq v_0 + 2v_1 + 3v_2$ . We can rewrite each such monomial uniquely in

terms of the ambient coordinates on  $\mathbb{P}^8$ , namely as a monomial that does not lie in the ideal (19). This monomial equals  $a_0^{\nu_{00}} a_1^{\nu_{01}} b_0^{\nu_{10}} b_1^{\nu_{11}} b_2^{\nu_{12}} c_0^{\nu_{20}} c_1^{\nu_{21}} c_2^{\nu_{22}} c_3^{\nu_{23}}$ . Its exponents satisfy  $\nu_{00} + \nu_{01} = \nu_0$ ,  $\nu_{10} + \nu_{11} + \nu_{12} = \nu_1$ ,  $\nu_{20} + \nu_{21} + \nu_{22} + \nu_{23} = \nu_2$  and  $\nu_{01} + \nu_{11} + 2\nu_{12} + \nu_{21} + 2\nu_{22} + 3\nu_{23} = i$ . For instance, if  $x^{\nu} = x_0^3 x_1^2 x_2^2$  then its various distortions, for  $0 \leq i \leq 13$ , are the monomials

$$a_0^3 b_0^2 c_0^2, a_0^3 b_0^2 c_0 c_1, a_0^3 b_0^2 c_0 c_2, a_0^3 b_0^2 c_0 c_3, a_0^3 b_0^2 c_1 c_3, a_0^3 b_0^2 c_2 c_3, a_0^3 b_0^2 c_3^2, \\ a_0^3 b_0 b_1 c_3^2, a_0^3 b_0 b_2 c_3^2, a_0^3 b_1 b_2 c_3^2, a_0^3 b_2^2 c_3^2, a_0^2 a_1 b_2^2 c_3^2, a_0 a_1^2 b_2^2 c_3^2, a_1^3 b_2^2 c_3^2.$$

Given any homogeneous polynomial  $p$  in the unknowns  $x_0, x_1, \dots, x_n$ , we write  $p_{[i]}$  for the polynomial on  $\mathbb{P}^N$  that is obtained by replacing each monomial in  $p$  by its  $i$ th distortion.

*Example 3.9* For the scroll in Example 2.1, the distortions of the sextic  $p = a^6 + a^2 b^2 c^2$  are

$$p_{[0]} = a_0^6 + a_0^2 b_0^2 c_0^2, \quad p_{[1]} = a_0^5 a_1 + a_0 a_1 b_0^2 c_0^2, \quad \dots, \quad p_{[5]} = a_0 a_1^5 + a_1^2 b_1 b_2 c_0^2, \\ p_{[6]} = a_1^6 + a_1^2 b_2^2 c_0^2, \dots$$

The following result shows how the equations of  $X_{[u]}$  can be read off from those of  $X$ .

**Theorem 3.10** *The ideal of the distortion variety  $X_{[u]}$  is generated by the  $\binom{N-n}{2}$  quadrics that define  $\mathcal{S}_u$  together with the distortions  $p_{[i]}$  of the elements  $p$  in the reduced Gröbner basis of  $X$  for a term order that refines the weights  $-u$ . Hence, the ideal is generated by polynomials whose degree is at most the maximal degree of any monomial generator of  $M = \text{in}_{-u}(X)$ .*

*Proof* Since  $X_{[u]} \subset \mathcal{S}_u$ , the binomial quadrics that define  $\mathcal{S}_u$  lie in the ideal  $I(X_{[u]})$ . Also, if  $p$  is a polynomial that vanishes on  $X$  then all of its distortions  $p_{[i]}$  are in  $I(X_{[u]})$  because

$$p_{[i]}(x_0, \lambda x_0, \dots, \lambda^{u_0} x_0, x_1, \dots, \lambda^{u_n} x_n) = \lambda^i \cdot p(x) = 0 \quad \text{for } \lambda \in \mathbb{C} \quad \text{and } x \in X.$$

Conversely, consider any homogeneous polynomial  $F$  in  $I(X_{[u]})$ . It must be shown that  $F$  is a polynomial linear combination of the specified quadrics and distortion polynomials. Without loss of generality, we may assume that  $F$  is standard with respect to the Gröbner basis in Lemma 3.6 and that each monomial in  $F$  has the same weight  $i$ . This implies

$$F(x_0, \lambda x_0, \dots, \lambda^{u_0} x_0, x_1, \dots, \lambda^{u_n} x_n) = \lambda^i f(x)$$

for some homogeneous  $f \in \mathbb{C}[x_0, \dots, x_n]$ . Since  $F \in I(X_{[u]})$ , we have  $f \in I(X)$ . We note also that  $F$  can be recovered from  $f$ , by applying the uniqueness part of Lemma 3.7 to each monomial in  $f$ . This implies that  $F = f_{[i]}$  equals the  $i$ th distortion of  $f$ .

We now write

$$f = h_1 p_1 + h_2 p_2 + \cdots + h_k p_k,$$

where  $p_1, p_2, \dots, p_k$  are in the reduced Gröbner basis of  $I(X)$  with respect to a term order refining  $-u$ , and the multipliers satisfy  $\deg_{-u}(f) \geq \deg_{-u}(h_j p_j) = \deg_{-u}(h_j) + \deg_{-u}(p_j)$  for  $j = 1, 2, \dots, k$ . Since  $F = f_{[i]}$ , we have  $-\deg_{-u}(f) \geq i$ . Hence, for each  $j$  there exist nonnegative integers  $a_j$  and  $b_j$  such that  $a_j + b_j = i$  and  $-\deg_{-u}(h_j) \geq a_j$  and  $-\deg_{-u}(p_j) \geq b_j$ . The latter inequalities imply that the distortion polynomials  $(h_j)_{[a_j]}$  and  $(p_j)_{[b_j]}$  exist.

Now consider the following polynomial in the coordinates on  $\mathbb{P}^N$ :

$$\tilde{F} = (h_1)_{[a_1]} \cdot (p_1)_{[b_1]} + \cdots + (h_k)_{[a_k]} \cdot (p_k)_{[b_k]}.$$

By construction,  $\tilde{F}$  and  $F$  both map to  $\lambda^i f$  under the parametrization of the scroll  $\mathcal{S}_u$ . Thus,  $\tilde{F} - F \in I(\mathcal{S}_u)$ . This shows that  $F$  is a polynomial linear combination of generators of  $I(\mathcal{S}_u)$  and distortions of Gröbner basis elements  $p_1, \dots, p_k$ . This completes the proof. □

We illustrate this result with two examples.

*Example 3.11* If  $X$  is a hypersurface of degree  $d \geq 2$ , then the ideal  $I(X_{[u]})$  is generated by binomial quadrics and distortion polynomials of degree  $d$ . More generally, if the generators of  $I(X)$  happen to be a Gröbner basis for  $-u$ , then the degree of the generators of  $I(X_{[u]})$  does not go up. This happens for all the varieties from computer vision seen in Sect. 2.

In general, however, the maximal degree among the generators of  $I(X_{[u]})$  can be much larger than that same degree for  $I(X)$ . This happens for complete intersection curves in  $\mathbb{P}^3$ :

*Example 3.12* Let  $X$  be the curve in  $\mathbb{P}^3$  obtained as the intersection of two random surfaces of degree 4. We fix  $u = (2, 3, 4, 4)$ . The initial ideal  $M = \text{in}_{-u}(X)$  has 51 monomial generators. The largest degree is 32. We now consider the distortion surface  $X_{[u]}$  in  $\mathbb{P}^{12}$ . The ideal of  $I(X_{[u]})$  is minimally generated by 133 polynomials. The largest degree is 32.

### 4 Multi-parameter Distortions

In this section, we study multi-parameter distortions of a given projective variety  $X \subset \mathbb{P}^n$ . Now,  $\lambda = (\lambda_1, \dots, \lambda_r)$  is a vector of  $r$  parameters, and  $u = (u_0, \dots, u_n)$  where  $u_i = \{u_{i,1}, u_{i,2}, \dots, u_{i,s_i}\}$  is an arbitrary finite subset of  $\mathbb{N}^r$ . Each point  $u_{i,j}$  represents a monomial in the  $r$  parameters, denoted  $\lambda^{u_{i,j}}$ . We set  $|u| = \sum_{i=0}^n |u_i| = \sum_{i=0}^n s_i$  and  $N = |u| - 1$ . The role of the scroll is played by a toric variety  $\mathcal{C}_u$  of dimension  $n + r$  in  $\mathbb{P}^N$  that is usually not smooth. Generalizing (10), we define the *Cayley variety*  $\mathcal{C}_u$  in  $\mathbb{P}^N$  by the parametrization

$$(x_0\lambda^{u_{0,1}} : x_0\lambda^{u_{0,2}} : \dots : x_0\lambda^{u_{0,s_0}} : x_1\lambda^{u_{1,1}} : \dots : x_1\lambda^{u_{1,s_1}} : \dots : x_r\lambda^{u_{r,1}} : \dots : x_r\lambda^{u_{r,s_r}}).$$
(20)

The name was chosen because  $C_u$  is the toric variety associated with the Cayley configuration of the configuration  $u$ . Its convex hull is the *Cayley polytope*; see [11, Section 3] and [27, Definition 4.6.1].

The distortion variety  $X_{[u]}$  is defined as the closure of the set of all points (20) in  $\mathbb{P}^N$  where  $x \in X$  and  $\lambda \in (\mathbb{C}^*)^r$ . Hence  $X_{[u]}$  is a subvariety of the Cayley variety  $C_u$ , typically of dimension  $d + r$  where  $d = \dim(X)$ . Note that, even in the single-parameter setting ( $r = 1$ ), we have generalized our construction, by permitting  $u_i$  to not be an initial segment of  $\mathbb{N}$ .

*Example 4.1* Let  $r = n = 2$ ,  $u_0 = \{(0, 0), (0, 1)\}$ ,  $u_1 = \{(0, 0), (1, 0)\}$ ,  $u_2 = \{(2, 2), (1, 1)\}$ . The Cayley variety  $C_u$  is the singular hypersurface in  $\mathbb{P}^5$  defined by  $a_0b_0c_0 - a_1b_1c_1$ . Let  $X$  be the conic in  $\mathbb{P}^2$  given by  $x_0^2 + x_1^2 - x_2^2$ . The distortion variety  $X_{[u]}$  is a threefold of degree 10. Its ideal is  $(a_0b_0c_0 - a_1b_1c_1, a_0^2c_0^2 + b_0^2c_0^2 - c_1^4, a_0^2a_1b_1c_0 + a_1b_0^2b_1c_0 - a_0b_0c_1^3, a_0^2a_1^2b_1^2 + a_1^2b_0^2b_1^2 - a_0^2b_0^2c_1^2)$ .

### 4.1 Two Views with Two or Four Distortion Parameters

We now present some motivating examples from computer vision. Multi-dimensional distortions arise when several cameras have different unknown radial distortions, or when the distortion function  $g(t) = 1 + \mu t^2$  in (4)–(5) is replaced by a polynomial of higher degree.

We return to the setting of Sect. 2, and we introduce two distinct distortion parameters  $\lambda_1$  and  $\lambda_2$ , one for each of the two cameras. The role of the equation (6) is played by

$$0 = \begin{pmatrix} U_2 \\ 1 + \lambda_2 \|U_2\|^2 \end{pmatrix}^\top \begin{bmatrix} x_{11} & x_{12} & x_{13} \\ x_{21} & x_{22} & x_{23} \\ x_{31} & x_{32} & x_{33} \end{bmatrix} \begin{pmatrix} U_1 \\ 1 + \lambda_1 \|U_1\|^2 \end{pmatrix}.$$
(21)

Just like in (9), this translates into one linear equation  $c^\top m = 0$ , where now  $m^\top = [x_{11}, x_{12}, x_{13}, \lambda_1 x_{13}, x_{21}, x_{22}, x_{23}, \lambda_1 x_{23}, x_{31}, x_{31}\lambda_2, x_{32}, x_{32}\lambda_2, x_{33}, x_{33}\lambda_2, x_{33}\lambda_1, x_{33}\lambda_1\lambda_2]$  and  $c^\top$  equals

$$\left[ u_2u_1, u_2v_1, u_2, u_2\|U_1\|^2, v_2u_1, v_2v_1, v_2, v_2\|U_1\|^2, u_1, u_1\|U_2\|^2, v_1, v_1\|U_2\|^2, 1, \|U_1\|^2, \|U_2\|^2, \|U_1\|^2\|U_2\|^2 \right].$$

Here  $c$  is a real vector of data, whereas  $\lambda = (\lambda_1, \lambda_2)$  and  $x = (x_{ij})$  comprise 11 unknowns. The vector  $m$  is a monomial parameterization of the form (20). The corresponding configuration  $u$  is given by  $u_{11} = u_{12} = u_{21} = u_{22} = \{(0, 0)\}$ ,  $u_{13} = u_{23} = \{(0, 0), (1, 0)\}$ ,  $u_{31} = u_{32} = \{(0, 0), (0, 1)\}$  and  $u_{33} = \{(0, 0), (1, 0), (0, 1), (1, 1)\}$ .

**Table 2** Dims, degrees, mingens of two-view models and their two-parameter radial distortions

	$\dim(X),$ $\deg(X)$	$\dim(X_{[u]})$	$\deg(X_{[u]})$	Proposition 3.1 iterated	# ideal gens of deg 2, 3, 4, 5
$\mathcal{F}$ in Example 1.1: $\lambda_1 + F + \lambda_2$	7, 3	9	24	36	11, 4, 0, 0
$\mathcal{E}$ in Example 2.2: $\lambda_1 + E + \lambda_2$	5, 10	7	76	120	11, 20, 0, 0
$\mathcal{G}$ in Example 2.3: $\lambda_1 f + E + f\lambda_2$	6, 15	8	104	180	11, 4, 0, 4
$\mathcal{G}'$ in Example 2.4: $\lambda_1 + E + f\lambda_2$	6, 9	8	56	108	11, 4, 15, 0

The Cayley variety  $\mathcal{C}_u$  lives in  $\mathbb{P}^{15}$ . It has dimension 10 and degree 10. Its toric ideal is generated by 11 quadratic binomials.

Let  $X \subset \mathbb{P}^8$  be one of the two-view models  $\mathcal{F}, \mathcal{E}, \mathcal{G}$ , or  $\mathcal{G}'$  in Sect. 2.3. The following table concerns the distortion varieties  $X_{[u]}$  in  $\mathbb{P}^{15}$ . It is an extension of Table 1.

On each  $X_{[u]}$ , we consider linear systems of equations  $c^\top m = 0$  that arise from point correspondences. For a minimal problem, the number of such epipolar constraints is  $\dim(X_{[u]})$ , and the expected number of its complex solutions is  $\deg(X_{[u]})$ . The last column summarizes the number of minimal generators of the ideal of  $X_{[u]}$ . For instance, the variety  $X_{[u]} = \mathcal{E}_{[u]}$  for essential matrices is defined by 11 quadrics (from  $\mathcal{C}_u$ ), 20 cubics, 0 quartics and 0 quintics. If we add 7 general linear equations to these then we have a system with 76 solutions in  $\mathbb{P}^{15}$ . The penultimate column of Table 2 gives an upper bound on  $\deg(X_{[u]})$  that is obtained by applying Proposition 3.1 twice, after decomposing  $u$  into two one-parameter distortions.

We next discuss four-parameter distortions for two cameras. These are based on the following model for epipolar constraints, which is a higher-order version of Eq. (21):

$$0 = \left( \begin{matrix} U_2 \\ 1 + \lambda_2 \|U_2\|^2 + \mu_2 \|U_2\|^4 \end{matrix} \right)^\top \begin{bmatrix} x_{11} & x_{12} & x_{13} \\ x_{21} & x_{22} & x_{23} \\ x_{31} & x_{32} & x_{33} \end{bmatrix} \left( \begin{matrix} U_1 \\ 1 + \lambda_1 \|U_1\|^2 + \mu_1 \|U_1\|^4 \end{matrix} \right). \tag{22}$$

As before, the  $3 \times 3$ -matrix  $x = (x_{ij})$  belongs to a two-view camera model  $\mathcal{E}, \mathcal{F}, \mathcal{G}$  or  $\mathcal{G}'$ . We rewrite (22) as the inner product  $c^\top m = 0$  of two vectors, where  $c$  records the data and  $m$  is a parametrization for the distortion variety. We now have  $n = 9, r = 4$  and  $|u| = 25$ . The configurations in  $\mathbb{N}^4$  that furnish the degrees for this four-parameter distortion are

$$\begin{aligned} u_{11} = u_{12} = u_{21} = u_{22} &= \{\mathbf{0}\}, \\ u_{13} = u_{23} &= \{\mathbf{0}, (1, 0, 0, 0), (0, 0, 1, 0)\}, u_{31} = u_{32} = \{\mathbf{0}, (0, 1, 0, 0), (0, 0, 0, 1)\}, \\ u_{33} &= \{\mathbf{0}, (1, 0, 0, 0), (0, 1, 0, 0), (0, 0, 1, 0), (0, 0, 0, 1), (1, 0, 1, 0), (1, 0, 0, 1), (0, 1, 1, 0), (0, 1, 0, 1)\}. \end{aligned}$$

Each of the resulting distortion varieties  $X_{[u]}$  lives in  $\mathbb{P}^{24}$  and satisfies  $\dim(X_{[u]}) = \dim(X) + 4$ . As before, we may compute the prime ideals for these distortion varieties by elimination, for instance in Macaulay2. From this, we obtain the information displayed in Table 3.

In each case, the 51 quadrics are binomials that define the ambient Cayley variety  $\mathcal{C}_u$  in  $\mathbb{P}^{24}$ . The minimal problems are now more challenging than those in Tables 1 and 2.

**Table 3** Dimension, degrees, number of minimal generators for four-parameter radial distortions

	Dimension	Degree	Quadratics	Cubics	Quartics	Quintics
$\mathcal{F}$ in Example 1.1: $\lambda_1\mu_1 + F + \lambda_2\mu_2$	11	115	51	9		
$\mathcal{E}$ in Example 2.2: $\lambda_1\mu_1 + E + \lambda_2\mu_2$	9	354	51	34		
$\mathcal{G}$ in Example 2.3: $\lambda_1\mu_1 f + E + f\lambda_2\mu_2$	10	245	51	9	42	
$\mathcal{G}'$ in Example 2.4: $\lambda_1\mu_1 + E + f\lambda_2\mu_2$	10	475	51	9		9

For instance, to recover the essential matrix along with four distortion parameters from 9 general point correspondences, we must solve a polynomial system that has 354 complex solutions.

### 4.2 Iterated Distortions and Their Tropicalization

In what follows we take a few steps toward a geometric theory of multi-parameter distortions. We begin with the observation that multi-parameter distortions arising in practice, including those in Sect. 4.1, will often have an inductive structure. Such a structure allows us to decompose them as successive one-parameter distortions where the degrees form an initial segment of the nonnegative integers  $\mathbb{N}$ . In that case, the results of Sect. 2 can be applied iteratively. The following proposition characterizes when this is possible. For  $u_i \subset \mathbb{N}^r$  and  $k < r$ , we write  $u_i|_{\mathbb{N}^k} \subset \mathbb{N}^k$  for the projection of the set  $u_i$  onto the first  $k$  coordinates.

**Proposition 4.2** *Let  $u = (u_0, \dots, u_n)$  be a sequence of finite nonempty subsets of  $\mathbb{N}^r$ . The multi-parameter distortion with respect to  $u$  in  $\lambda_1, \dots, \lambda_r$  is a succession of one-parameter distortions by initial segments, in  $\lambda_1$ , then  $\lambda_2$ , and so on, if and only if each fiber of the maps  $u_i|_{\mathbb{N}^k} \rightarrow u_i|_{\mathbb{N}^{k-1}}$  becomes an initial segment of  $\mathbb{N}$  when projected onto the  $k^{\text{th}}$  coordinate. This condition holds when each  $u_i$  is an order ideal in the poset  $\mathbb{N}^r$ , with coordinate-wise order.*

*Proof* We show this for  $r = 2$ . The general case is similar but notationally more cumbersome. The two-parameter distortion given by a sequence  $u$  decomposes into two one-parameter distortions if and only if there exist vectors  $v = (v_0, \dots, v_n) \in \mathbb{N}^{n+1}$  and  $w = (w_0, \dots, w_n) \in \mathbb{N}^{v_0+1} \oplus \dots \oplus \mathbb{N}^{v_n+1}$  such that  $u_i = \{(s, t) : 0 \leq s \leq v_i \text{ and } 0 \leq t \leq w_{is}\}$  for  $i = 0, 1, \dots, n$ . This means that both the Cayley variety and any distortion subvariety decompose as follows:

$$\mathcal{C}_u = (\mathcal{S}_v)_{[w]} \quad \text{and} \quad X_{[u]} = (X_{[v]})_{[w]}. \tag{23}$$

The segment  $[0, v_i]$  in  $\mathbb{N}$  is the unique fiber of the map  $u_i|_{\mathbb{N}^1} \rightarrow u_i|_{\mathbb{N}^0} = \{0\}$ . The fiber of  $u_i|_{\mathbb{N}^2} \rightarrow u_i|_{\mathbb{N}^1} = [0, v_i]$  over an integer  $s$  is the segment  $[0, w_{is}]$  in  $\mathbb{N}$ . Thus the stated condition on fibers is equivalent to the existence of the nonnegative integers  $v_i$  and  $w_{is}$ . For the second claim, we note that the set  $u_i$  is an order ideal in  $\mathbb{N}^2$  precisely when  $w_{i0} \geq w_{i1} \geq \dots \geq w_{is}$ .  $\square$

Proposition 4.2 applies to all models seen in Sect. 4.1 since the  $u_i$  are order ideals.

*Example 4.3* Consider the two-parameter radial distortion model for two cameras derived in (21). The vectors in the above proof are  $v = (0, 0, 1, 0, 0, 1, 0, 0, 1)$  and  $w = (0, 0, (0, 0), 0, 0, (0, 0), 1, 1, (1, 1))$ . The decomposition (23) holds for all four models  $X = \mathcal{E}, \mathcal{F}, \mathcal{G}, \mathcal{G}'$ . The penultimate column of Table 2 says that the degree of  $(X_{[v]})_{[w]}$  is bounded above by  $12 \cdot \deg(X)$ . This follows directly from Proposition 3.1 because  $12 = |v| \cdot |w|$ .

The exact degrees for  $X_{[u]}$  shown in Tables 2 and 3 were found using Gröbner bases. This computation starts from the ideal of  $X$  and incorporates the structure in Proposition 4.2.

*Tropical geometry* [27] furnishes tools for studying multi-parameter distortion varieties. In what follows we identify any variety  $X \subset \mathbb{P}^n$  with its reembedding into  $\mathbb{P}^N$ , where the  $i$ -th coordinate  $x_i$  has been duplicated  $|u_i|$  times. Consider the distortion variety  $\mathbf{1}_{[u]}$  of the point  $\mathbf{1} = (1 : 1 : \dots : 1)$  in  $\mathbb{P}^n$ . This is the toric variety in  $\mathbb{P}^N$  given by the parametrization

$$(\lambda^{u_{0,1}} : \lambda^{u_{0,2}} : \dots : \lambda^{u_{0,s_0}} : \lambda^{u_{1,1}} : \dots : \lambda^{u_{1,s_1}} : \dots : \lambda^{u_{r,1}} : \dots : \lambda^{u_{r,s_r}}) \text{ for } \lambda \in (\mathbb{C}^*)^{r+1}.$$

Let  $\tilde{u}$  denote the  $(r+1) \times (N+1)$ -matrix whose columns are vectors in the sets  $u_i$  for  $i = 0, 1, \dots, n$ , augmented by an extra all-one row vector  $(1, 1, \dots, 1)$ . This matrix represents the toric variety  $\mathbf{1}_{[u]}$ . Recall that the *Hadamard product*  $\star$  of two vectors in  $\mathbb{C}^{n+1}$  is their coordinate-wise product. This operation extends to points in  $\mathbb{P}^n$  and also to subvarieties.

**Theorem 4.4** Fix a projective variety  $X \subset \mathbb{P}^n$  and any distortion system  $u$ , regarded as  $r \times (N + 1)$ -matrix. The distortion variety is the Hadamard product of  $X$  with a toric variety:

$$X_{[u]} = X \star \mathbf{1}_{[u]}$$

Its tropicalization is the Minkowski sum of the tropicalization of  $X$  with a linear space:

$$\text{trop}(X_{[u]}) = \text{trop}(X) + \text{trop}(\mathbf{1}_{[u]}) = \text{trop}(X) + \text{rowspan}(\tilde{u}). \tag{24}$$

*Proof* This follows from Eq. (20) and [27, Chapter 5]. The toric variety  $\mathbf{1}_{[u]}$  in  $\mathbb{P}^N$  is represented by the matrix  $\tilde{u}$ , in the sense of [34], so its tropicalization is the row space of  $\tilde{u}$ . Tropicalization takes Hadamard products into Minkowski sums, by [2, Propostion 5.1] or [27, Proposition 5.5.11].  $\square$

Theorem 4.4 suggests the following method for computing degrees of multi-parameter distortion varieties. Let  $L$  be the standard tropical linear space of codimension  $r + \dim(X)$  in  $\mathbb{R}^{N+1}/\mathbb{R}\mathbf{1}$ , as in [27, Corollary 3.6.16]. Fix a general point  $\xi$  in  $\mathbb{R}^{N+1}/\mathbb{R}\mathbf{1}$ . Then  $\deg(X_{[u]})$  is the number of points, counted with multiplicity, in the intersection of the tropical variety (24) with the tropical linear space  $\xi + L$ . In practice,  $X$  is fixed and we precompute  $\text{trop}(X)$ . That fan then gets intersected with  $\xi + L + \text{rowspan}(\tilde{u})$  for various configurations  $u$ .

**Table 4** Tropical varieties in  $\mathbb{R}^0/\mathbb{R}\mathbf{1}$  associated with the two-view models

Variety $X$	Dim	Lineality	f-vector	Multiplicities
$\mathcal{F}$ in Example 1.1	7	4	(9, 18, 15)	$1_{15}$
$\mathcal{E}$ in Example 2.2	5	0	(591, 4506, 12,588, 15,102, 6498)	$2_{6426}, 4_{72}$
$\mathcal{G}$ in Example 2.3	6	1	(32, 213, 603, 780, 390)	$1_{336}, 2_{54}$
$\mathcal{G}'$ in Example 2.4	6	1	(100, 746, 2158, 2800, 1380)	$1_{800}, 2_{572}, 4_8$

**Corollary 4.5** *The degree of  $X_{[u]}$  is a piecewise-linear function in the maximal minors of  $\tilde{u}$ .*

*Proof* The maximal minors of  $\tilde{u}$  are the Plücker coordinates of the row space of  $\tilde{u}$ . An argument as in [7, Section 4] leads to a polyhedral chamber decomposition of the relevant Grassmannian, according to which pairs of cones in  $\text{trop}(X)$  and in  $\xi + L + \text{rowspace}(\tilde{u})$  actually intersect. Each such intersection is a point, and its multiplicity is one of the maximal minors of  $\tilde{u}$ .  $\square$

Using the software *Gfan* [21], we precomputed the tropical varieties  $\text{trop}(X)$  for our four basic two-view models, namely  $X = \mathcal{E}, \mathcal{F}, \mathcal{G}, \mathcal{G}'$ . The results are summarized in Table 4.

The lineality space corresponds to a torus action on  $X$ . Its dimension is given in column 2. Modulo this space,  $\text{trop}(X)$  is a pointed fan. Column 3 records the number of  $i$ -dimensional cones for  $i = 1, 2, 3, \dots$  Each maximal cone comes with an integer multiplicity [27, Section 3.4]. These multiplicities are 1, 2 or 4 for our examples. Column 4 indicates their distribution.

### 5 Application to Minimal Problems

This section offers a case study for one *minimal problem* which has not yet been treated in the computer vision literature. We build and test an efficient Gröbner basis solver for it. Our approach follows [25, 26] and applies in principle to any zero-dimensional parametrized polynomial system. This illustrates how the theory in Sects. 2, 3, 4 ties in with practice.

We fix the distortion variety  $f + E + \lambda$  in Table 1. This is the variety  $\mathcal{G}''_{[v]}$  which lives in  $\mathbb{P}^{11}$  and has dimension 7 and degree 23. We represent its defining equations by the matrix

$$\begin{pmatrix} x_{11} & x_{12} & x_{21}x_{31} + x_{22}x_{32} + x_{23}x_{33} & x_{13} & y_{13} \\ x_{21} & x_{22} & -x_{11}x_{31} - x_{12}x_{32} - x_{13}x_{33} & x_{23} & y_{23} \\ x_{31} & x_{32} & 0 & x_{33} & y_{33} \end{pmatrix}. \tag{25}$$

This matrix is derived by augmenting (13) with the  $y$ -column. The prime ideal of  $\mathcal{G}''_{[v]}$  is generated by all  $3 \times 3$ -minors of (25) and the  $2 \times 2$ -minors in the last two columns. The real points on this projective variety represent the relative position of two cameras, one with an unknown focal length  $f$  and the other with an unknown radial distortion parameter  $\lambda$ .

Each pair  $(U_1, U_2)$  of image points gives a constraint (6) which translates into a linear equation on  $\mathcal{G}''_{[v]} \cap L' \subset \mathbb{P}^{11}$ , as in Eq. (9). Here  $m^\top = [x_{11}, x_{12}, x_{13}, y_{13}, x_{21}, x_{22}, x_{23}, y_{23}, x_{31}, x_{32}, x_{33}, y_{33}]$  is the vector of unknowns. Using notation as in Sect. 2.1, the coefficient vector of the equation  $c^\top m = 0$  is  $c^\top = [u_2 u_1, u_2 v_1, u_2, u_2 \|U_1\|^2, v_2 u_1, v_2 v_1, v_2, v_2 \|U_1\|^2, u_1, v_1, 1, \|U_1\|^2]$ .

Seven pairs determine a linear system  $Cm = 0$  where the coefficient matrix  $C$  has format  $7 \times 12$ . For general data, the matrix  $C$  has full rank 7. The solution set is a 5-dimensional linear subspace in  $\mathbb{R}^{12}$ , or, equivalently, a 4-dimensional subspace  $L'$  in  $\mathbb{P}^{11}$ . The intersection  $\mathcal{G}''_{[v]} \cap L'$  consists of 23 points. Our aim is to compute these fast and accurately. This is what is meant by the *minimal problem* associated with the distortion variety  $\mathcal{G}''_{[v]}$ .

### 5.1 First Build Elimination Template, then Solve Instances Very Fast

We shall employ the method of *automatic generation of Gröbner solvers*. This has already been applied with considerable success to a wide range of camera geometry problems in computer vision; see e.g., [25,26]. We start by computing a suitable basis  $\{n_1, n_2, n_3, n_4, n_5\}$  for the null space of  $C$  in  $\mathbb{R}^{12}$ . We then introduce four unknowns  $\gamma_1, \dots, \gamma_4$ , and we substitute

$$m = \gamma_1 n_1 + \gamma_2 n_2 + \gamma_3 n_3 + \gamma_4 n_4 + n_5. \tag{26}$$

Our rank constraints on (25) translate into ten equations in  $\gamma_1, \gamma_2, \gamma_3, \gamma_4$ . This system has 23 solutions in  $\mathbb{C}^4$ . Our aim is to compute these within a few tens or hundreds of *microseconds*.

Efficient and stable Gröbner solvers are often based on *Stickelberger's Theorem* [35, Theorem 2.6], which expresses the solutions as the joint eigenvalues of its companion matrices. Let  $I \subset \mathbb{R}[\gamma]$  be the ideal generated by our ten polynomials in  $\gamma = (\gamma_1, \gamma_2, \gamma_3, \gamma_4)$ . The quotient ring  $\mathbb{R}[\gamma]/I$  is isomorphic to  $\mathbb{R}^{23}$ . An  $\mathbb{R}$ -vector space basis  $B$  is given by the standard monomials with respect to any Gröbner basis of  $I$ . The multiplication map  $M_i : \mathbb{R}[\gamma]/I \rightarrow \mathbb{R}[\gamma]/I, f \mapsto f\gamma_i$  is  $\mathbb{R}$ -linear. Using the basis  $B$ , this becomes a  $23 \times 23$ -matrix. The matrices  $M_1, M_2, M_3, M_4$  commute pairwise. These are the *companion matrices*. As an  $\mathbb{R}$ -algebra,  $\mathbb{R}[M_1, M_2, M_3, M_4] \simeq \mathbb{R}[\gamma]/I$ . Since  $I$  is radical, there are 23 linearly independent joint eigenvectors  $\mathbf{x}$ , satisfying  $M_i \mathbf{x} = \lambda_i \mathbf{x}$ . The vectors  $(\lambda_1, \lambda_2, \lambda_3, \lambda_4) \in \mathbb{C}^4$  are the zeros of  $I$ .

In practice, it suffices to construct only one of the companion matrices  $M_i$ , since we can recover the zeros of  $I$  from eigenvectors  $\mathbf{x}$  of  $M_i$ . Thus, our primary task is to compute either  $M_1, M_2, M_3$  or  $M_4$  from seven point correspondences  $(U_1, U_2)$  in a manner that is both very fast and numerically stable. For this purpose, the *automatic generator* of Gröbner solvers [25,26] is used. We now explain this method and illustrate it for the  $f + E + \lambda$  problem.

To achieve speed in computation, we exploit that, for generic data, Buchberger's algorithm always rewrites the input polynomials in the same way. The resulting Gröbner trace [36] is always the same. Therefore, we can construct a single trace for all generic systems by tracing the construction of a Gröbner basis of a single "generic"

system. This is done only once in an *offline* stage of solver generation. It produces an *elimination template*, which is then reused again and again for efficient *online* computations on generic data.

Starting with the input polynomial system  $\mathbf{F} = \{f_1, \dots, f_{10}\}$ , the *offline* part of the solver generation is a variant of the Gröbner trace algorithm in [36]. Based on the F4 algorithm [13] for a particular generic system, it produces an elimination template for constructing a Gröbner basis of  $\langle \mathbf{F} \rangle$ . The system  $\mathbf{F} = \{f_1, \dots, f_{10}\}$  is written in the form  $A m = 0$ , where  $A$  is the matrix of coefficients and  $m$  is the vectors of monomials of the system. Every Gröbner basis  $\mathbf{G}$  of  $\mathbf{F}$  can be constructed by Gauss–Jordan (G–J) elimination of a coefficient matrix  $A_d$  derived from  $\mathbf{F}$  by multiplying each polynomial  $f_i \in \mathbf{F}$ , by all monomials up to degree  $\max\{0, d - d_i\}$ , where  $d_i = \deg(f_i)$ .

To find an appropriate  $d$ , our solver generator starts with  $d = \min\{d_i\}$ , sets  $m_d = m$ , and G–J eliminates the matrix  $A_{\min\{d_i\}} = A$ . Then, it checks if a Gröbner basis  $\mathbf{G}$  has been generated. If not, it increases  $d$  by one, builds the next  $A_d$  and  $m_d$ , and goes back to the check. This is repeated until a suitable  $d$  and a Gröbner basis  $\mathbf{G}$  has been found. Often, we can remove some rows (polynomials) from  $A_d$  at this stage and form a smaller elimination template, denoted  $A'_d$ . For this, another heuristic optimization procedure is employed, aimed at removing unnecessary polynomials and provide an efficient template leading from  $\mathbf{F}$  to the reduced coefficient matrix  $A'_d$ . For a detailed description see [26] and [25, Section 4.4.3].

In order to guide this process, we first precompute the reduced Gröbner basis of  $I$ , e.g., w.r.t. grevlex ordering in Macaulay2 [18], and the associated monomial basis  $B$  of  $\mathbb{R}[\gamma]/I$ . This has to be done in exact arithmetic over  $\mathbb{Q}$ , which is computationally very demanding, due to the coefficient growth [1]. We alleviate this problem by using modular arithmetic [13] or by computing directly in a finite field modulo a single “lucky prime number” [36]. For many practical problems [6, 30, 32], small primes like 30,011 or 30,013 are sufficient.

The output of this offline algorithm is the elimination template for constructing  $A'_d$ , i.e., the list of monomials multiplying each polynomial of  $\mathbf{F}$  to produce  $A'_d$  and  $m'_d$ . The template is encoded as manipulations of sparse coefficient matrices. After removing unnecessary rows and columns, the matrix  $A'_d$  has size  $s \times (s + |B|)$  for some  $s$ . The left  $s \times s$ -block is invertible. Multiplying  $A'_d$  by that inverse and extracting appropriate rows, one obtains the  $|B| \times |B|$  matrix  $M_1$  that represents the linear map  $\mathbb{R}[\gamma]/I \rightarrow \mathbb{R}[\gamma]/I, f \mapsto f\gamma_1$  in the basis  $B$ .

We applied this offline algorithm to the  $f + E + \lambda$  problem, with standard monomial basis

$$B = (1, \gamma_1, \gamma_1\gamma_3, \gamma_1\gamma_3\gamma_4, \gamma_1\gamma_4, \gamma_1\gamma_4^2, \gamma_2, \gamma_2\gamma_3, \gamma_2\gamma_3\gamma_4, \gamma_2\gamma_4, \gamma_2\gamma_4^2, \gamma_2\gamma_4^3, \gamma_3, \gamma_3^2, \gamma_3^3, \gamma_3^2\gamma_4, \gamma_3\gamma_4, \gamma_3\gamma_4^2, \gamma_3\gamma_4^3, \gamma_4, \gamma_4^2, \gamma_4^3, \gamma_4^4).$$

Note that  $|B| = 23$ . The matrix (25) gives the following ten ideal generators (with  $d_1=d_2=d_3=2, d_4=d_5=3, d_6=\dots=d_{10}=4$ ) for the variety  $\mathcal{G}'_{[u]}$  encoding the  $f + E + \lambda$  problem:

$$\begin{aligned}
 f_1 &= && y_{23}x_{33} - x_{23}y_{33} \\
 f_2 &= && y_{13}x_{33} - x_{13}y_{33} \\
 f_3 &= && y_{13}x_{23} - x_{13}y_{23} \\
 f_4 &= && y_{13}x_{22}x_{31} - x_{12}y_{23}x_{31} - y_{13}x_{21}x_{32} + x_{11}y_{23}x_{32} + x_{12}x_{21}y_{33} - x_{11}x_{22}y_{33} \\
 f_5 &= && x_{13}x_{22}x_{31} - x_{12}x_{23}x_{31} - x_{13}x_{21}x_{32} + x_{11}x_{23}x_{32} + x_{12}x_{21}x_{33} - x_{11}x_{22}x_{33} \\
 f_6 &= && x_{11}y_{13}x_{31}x_{32} + x_{21}y_{23}x_{31}x_{32} + x_{12}y_{13}x_{32}^2 + x_{22}y_{23}x_{32}^2 - x_{11}x_{12}x_{31}y_{33} - x_{21}x_{22}x_{31}y_{33} \\
 &&& - x_{12}^2x_{32}y_{33} + x_{13}^2x_{32}y_{33} - x_{22}^2x_{32}y_{33} + x_{23}^2x_{32}y_{33} - x_{12}x_{13}x_{33}y_{33} - x_{22}x_{23}x_{33}y_{33} \\
 &&& \dots \dots \dots \\
 f_{10} &= && x_{11}x_{12}x_{31}^2 + x_{21}x_{22}x_{31}^2 - x_{11}^2x_{31}x_{32} + x_{12}^2x_{31}x_{32} - x_{21}^2x_{31}x_{32} + x_{22}^2x_{31}x_{32} \\
 &&& - x_{11}x_{12}x_{32}^2 - x_{21}x_{22}x_{32}^2 + x_{12}x_{13}x_{31}x_{33} + x_{22}x_{23}x_{31}x_{33} - x_{11}x_{13}x_{32}x_{33} - x_{21}x_{23}x_{32}x_{33}
 \end{aligned}$$

Using (26), these are inhomogeneous polynomials in  $\gamma_1, \gamma_2, \gamma_3, \gamma_4$ . In the offline algorithm, we multiply  $f_i$  by all monomials up to degree  $5 - d_i$  in these four variables. Each of  $f_1, f_2, f_3$  is multiplied by the 35 monomials of degree  $\leq 3$ , each of  $f_4, f_5$  is multiplied by the 15 monomials of degree  $\leq 2$ , and each of  $f_6, \dots, f_{10}$  is multiplied by the 5 monomials of degree  $\leq 1$ . The resulting 160 = 10 + 105 + 30 + 25 polynomials are written as a matrix  $A_5$  with 160 rows. Only 103 rows are needed to construct the matrix  $M_1$ . We conclude with an elimination template matrix  $A'_5$  of format  $103 \times 126$ . For any data  $C$ , the online solver performs G–J elimination on that matrix, and it computes the eigenvectors of a  $23 \times 23$  matrix  $M_1$ .

To avoid coefficient growth in the online stage, exact computations over  $\mathbb{Q}$  are replaced by approximate computations with floating point numbers in  $\mathbb{R}$ . In a naive implementation, expected cancellations may fail to occur due to rounding errors, thus leading to incorrect results. This is not a problem in our method because we follow the precomputed elimination template: we use only matrix entries that were nonzero in the offline stage. Still, replacing the symbolic F4 algorithm with a numerical computation may lead to very unstable behavior.

It has been observed [3] that different formulations, term orderings, pair selection strategies, etc., can have a dramatic effect on the stability and speed of the final solver. It is hence crucial to validate every solver experimentally, by simulations as well as on real data.

### 5.2 Computational Results

A complete solution, in the engineering sense, to a minimal problem is a solution that is: (1) fast and (2) numerically stable for most of the data that occur in practice. Moreover, for applications it is important to study the distribution of real solutions of the minimal solver.

Minimal solvers are often used inside RANSAC style loops [14]. They form parts of much larger systems, such as structure-from-motion and 3D reconstruction pipelines or localization systems. Maximizing the efficiency of these solvers is an essential task. Inside a RANSAC loop, all real zeros returned by the solver are seen as possible solutions to the problem. The consistency w.r.t. all measurements is tested for each of them. Since that test may be computationally expensive, the study of the distribution of real solutions is important.

In this section, we present graphs and statistics that display properties of the complete solution we offer for the  $f + E + \lambda$  problem. We studied the performance of our Gröbner solver on synthetically generated 3D scenes with known ground-truth parameters. We generated 500,000 different scenes with 3D points randomly distributed in a cube  $[-10, 10]^3$  and cameras with random feasible poses. Each 3D point was projected by two cameras. The focal length  $f$  of the left camera was drawn uniformly from the interval  $[0.5, 2.5]$ , and the focal length of the right camera was set to 1. The orientations and positions of the cameras were selected at random so as to look at the scene from a random distance, varying from 20 to 40 from the center of the scene. Next, the image projections in the right camera were corrupted by random radial distortion, following the one-parameter division model in [15]. The radial distortion  $\lambda$  was drawn uniformly from the interval  $[-0.7, 0]$ . The aim was to investigate the behavior of the algorithms for large as well as small amounts of radial distortion.

*Computation and its speed.* The proposed  $f + E + \lambda$  solver performs the following steps:

1. Fill the  $103 \times 126$  elimination template matrix  $A'_5$  with coefficients derived from the input measurements.
2. Perform G–J elimination on the matrix  $A'_5$ .
3. Extract the desired coefficients from the eliminated matrix.
4. Create the multiplication matrix from extracted coefficients.
5. Compute the eigenvectors of the multiplication matrix.
6. Extract 23 complex solutions  $(\gamma_1, \gamma_2, \gamma_3, \gamma_4)$  from the eigenvectors.
7. For each real solution  $(\gamma_1, \gamma_2, \gamma_3, \gamma_4)$ , recover the monomial vector  $m$  as in (26), the fundamental matrix  $F$ , the focal length  $f$ , and the radial distortion  $\lambda$ .

These seven steps were implemented efficiently. The final  $f + E + \lambda$  solver runs in less than 1 ms. All computations reported in this section were performed on an Intel(R) Core(TM) i5-2520M CPU @ 2.50 GHz laptop.

*Numerical stability.* We studied the behavior of our solver on noise-free data. Figure 1a shows the distribution of  $\text{Log}_{10}$  of the relative error of the radial distortion parameter  $\lambda$  estimated using the new  $f + E + \lambda$  solver. These result were obtained by selecting the real roots closest to the ground-truth values. The results suggest that the solver delivers correct solutions and its numerical stability is suitable for real-word applications.

Figure 1b shows the distribution of  $\text{Log}_{10}$  of the relative error of the estimated focal length  $f$ . Again these result were obtained by selecting the real roots closest to the ground-truth values. Note that the  $f + E + \lambda$  solver does not directly compute the focal length  $f$ . Its output is the monomial vector in  $m$  (26), from which we extract  $\lambda$  and the fundamental matrix  $X = (x_{ij})$ . To obtain the unknown focal length from  $X$ , we use the following formula:

**Lemma 5.1** *Let  $X = (x_{ij})_{1 \leq i, j \leq 3}$  be a generic point in the variety  $\mathcal{G}''$  from Example 2.5. Then there are exactly two pairs of essential matrix and focal length  $(E, f)$  such that  $X = \text{diag}(f^{-1}, f^{-1}, 1)E$ . If one of them is  $(E, f)$  then the other is*

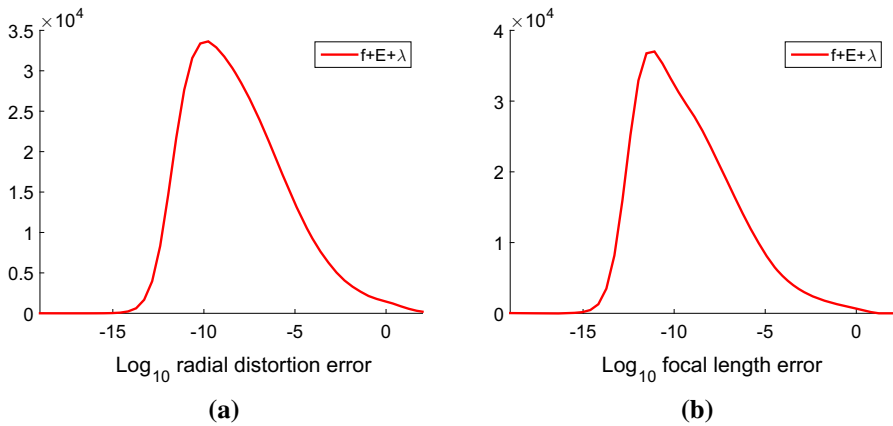


**Fig. 1** Numerical stability. **a**  $\text{Log}_{10}$  of the relative error of the estimated radial distortion. **b**  $\text{Log}_{10}$  of the relative error of the estimated focal length

$(\text{diag}(-1, -1, 1)E, -f)$ . In particular,  $f$  is determined up to sign by  $X$ . A formula to recover  $f$  from  $X$  is as follows:

$$f^2 = \frac{x_{23}x_{31}^2 + x_{23}x_{32}^2 - 2x_{21}x_{31}x_{33} - 2x_{22}x_{32}x_{33} - x_{23}x_{33}^2}{2x_{11}x_{13}x_{21} + 2x_{12}x_{13}x_{22} - x_{11}^2x_{23} - x_{12}^2x_{23} + x_{13}^2x_{23} + x_{21}^2x_{23} + x_{22}^2x_{23} + x_{23}^3}. \quad (27)$$

*Proof* Consider the map  $\mathcal{E} \times \mathbb{C}^* \rightarrow \mathbb{P}^8, (E, f) \mapsto \text{diag}(f^{-1}, f^{-1}, 1)E$ . Let  $I \subset \mathbb{Q}[e_{ij}, f, x_{ij}]$  be the ideal of the graph of this map, where  $E = (e_{ij})_{1 \leq i, j \leq 3}$ . So,  $I$  is generated by the ten D emazure cubics and the nine entries of  $X - \text{diag}(f^{-1}, f^{-1}, 1)E$ . We computed the elimination ideal  $I \cap \mathbb{Q}[f, x_{ij}]$  in Macaulay2. The polynomial gotten by clearing the denominator and subtracting the RHS from the LHS in the formula (27) lies in this elimination ideal.  $\square$

*Counting real solutions.* In the next experiment, we studied the distribution of the number of real solutions  $(\lambda, F)$  and the number of real solutions for the focal length  $f$ .

Figure 2a shows the histogram of the number of real solutions on the distortion variety  $\mathcal{G}''_{[v]}$ . All odd integers between 1 and 23 were observed. Most of the time we obtained an odd number of real solutions between 7 and 15. The empirical probabilities are in Table 5.

Figure 2b shows the histogram of the number of real solutions for the focal length  $f$ , computed from the distortion variety  $\mathcal{G}''_{[v]}$  using the formula (27). Of the 46 complex solutions, at most 23 could be real and positive. The largest number of positive real solutions  $f$  observed in 500,000 runs was 16. The empirical probabilities from this experiment are in Table 6.

We performed the same experiment with image measurements corrupted by Gaussian noise with the standard deviation set to 2 pixels. The distribution of the real roots in the distortion variety  $\mathcal{G}''_{[v]}$  was very similar to the distribution for noise-free data. The main difference between these result and those for noise-free data was in the number of real values for the focal length  $f$ . For a fundamental matrix corrupted by

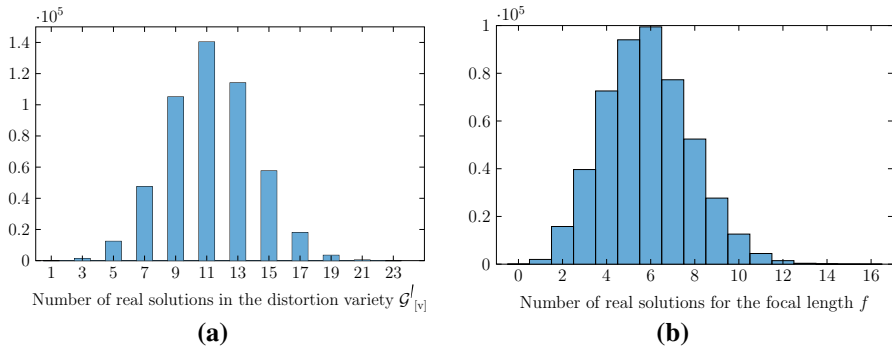


**Fig. 2** Number of real solutions for floating point computation with noise-free image data

**Table 5** Distribution of the number of real solutions in the distortion variety  $G''_{[v]}$  for noise-free data

Real roots in $G''_{[v]}$	1	3	5	7	9	11	13	15	17	19	21	23
%	0.003	0.276	2.47	9.50	21.0	28.0	22.8	11.5	3.60	0.681	0.078	0.003

**Table 6** Distribution of the number of positive real roots for the focal length  $f$  for noise-free data

Real $f$	0	1	2	3	4	5	6	7	8	9	10	11
%	0.003	0.397	3.16	7.93	14.5	18.8	19.9	15.5	10.5	5.54	2.52	0.894
Real $f$	12	13	14	15	16							
%	0.295	0.075	0.023	0.005	0.001							

**Table 7** Distribution of the number of real solutions in the distortion variety  $G''_{[v]}$  for image measurements corrupted with Gaussian noise with  $\sigma = 2$  pixels

Real roots	1	3	5	7	9	11	13	15	17	19	21	23
%	0.021	0.509	3.23	11.2	22.4	27.7	21.1	10.1	3.07	0.566	0.062	0.004

noise, the formula (27) results in no real solutions more often. See Tables 7 and 8 for the empirical probabilities.

Finally, we performed the same experiments for a special camera motion. It is known [29, 33] that the focal length cannot be determined by the formula (27) from the fundamental matrix if the optical axes are parallel to each other, e.g., for a sideways motion of cameras. Therefore, we generated cameras undergoing “close-to-sideways motion”. To model this scenario, 100 points were placed in a 3D cube  $[-10, 10]^3$ . Then 500,000 different camera pairs were generated such that both cameras were first pointed in the same direction (optical axes intersect at infinity) and then translated laterally. Next, a small amount of rotational noise of 0.01 degrees was introduced into the camera poses by right-multiplying the projection matrices by rotation matrices.

**Table 8** Distribution of the number of real roots for the focal length  $f$  with data as in Table 7

Real $f$	0	1	2	3	4	5	6	7	8	9	10	11
%	0.243	1.30	4.92	10.2	16.1	19.0	18.5	13.7	8.79	4.33	1.96	0.689
Real $f$	12	13	14	15	16							
%	0.217	0.048	0.015	0.002	0.001							

**Table 9** Distribution of the number of real solutions in the distortion variety  $\mathcal{G}''_{[v]}$  for the close-to-sideways motion scenario with noise-free data

Real roots	1	3	5	7	9	11	13	15	17	19	21	23
%	0.007	0.544	5.14	16.83	26.2	24.9	16.2	7.37	2.30	0.475	0.061	0.006

**Table 10** Distribution of the number of real solutions for the focal length  $f$  in the close-to-sideways motion scenario with noise-free data

Real $f$	0	1	2	3	4	5	6	7	8	9	10	11
%	0.006	0.755	3.08	10.2	12.9	20.9	16.2	16.0	8.73	6.17	2.61	1.58
Real $f$	12	13	14	15	16	17	18	19	20			
%	0.556	0.253	0.086	0.033	0.011	0.0044	0.0016	0.0012	0.0002			

This multiplication slightly rotated the optical axes of cameras (as not to intersect at infinity) as well as simultaneously displaced the camera centers.

The results for noise-free data are displayed in Tables 9 and 10. For this special close-to-sideways motion, the formula (27) provides up to 20 real solutions for the focal length  $f$ .

**Acknowledgements** This project started at the *Algebraic Vision* workshop (May 2016) at the American Institute of Mathematics (AIM) in San Jose. We are grateful to the organizers, Sameer Agarwal, Max Lieblich and Rekha Thomas, for bringing us together. Joe Kileel and Bernd Sturmfels were supported by the US National Science Foundation (DMS-1419018). Zuzana Kukelova was supported by the Czech Science Foundation (GACR P103/12/G084). Part of this study was carried out while she worked for Microsoft Research, Cambridge, UK. Tomas Pajdla was supported by H2020-ICT-731970 LADIO, the Robotics for Industry 4.0 Project CZ.02.1.01/0.0/0.0/15\_003/0000470 and the European Regional Development Fund.

## References

1. E. Arnold, *Modular algorithms for computing Gröbner bases*, J. Symbolic Comput. **35** (2003) 403–419.
2. C. Bocci, E. Carlini and J. Kileel, *Hadamard products of linear spaces*, J. Algebra **448** (2016) 595–617.
3. M. Bujnak, *Algebraic solutions to absolute pose problems*, Doctoral Thesis, Czech Technical University in Prague, 2012.
4. M. Bujnak, Z. Kukelova, and T. Pajdla, *3D reconstruction from image collections with a single known focal length*, in Proceedings of the 2009 IEEE International Conference on Computer Vision (ICCV 2009), pp. 351–358.

5. M. Bujnak, Z. Kukeleva and T. Pajdla, *Making minimal solvers fast*, in Proceedings of the 2012 IEEE Conference on Computer Vision and Pattern Recognition (CVPR 2012), pp. 1506–1513.
6. M. Byrod, Z. Kukeleva, K. Josephson, T. Pajdla and K. Åström, *Fast and robust numerical solutions to minimal problems for cameras with radial distortion*, in Proceedings of the 2008 IEEE Conference on Computer Vision and Pattern Recognition (CVPR 2008), pp. 1–8.
7. E. Cattani, M. A. Cueto, A. Dickenstein, S. Di Rocco and B. Sturmfels, *Mixed discriminants*, *Math. Z.* **274** (2013) 761–778.
8. D. Cox, J. Little and H. Schenck, *Toric varieties*, Graduate Studies in Mathematics **124**, American Mathematical Society, Providence, 2011.
9. J. Dalbec and B. Sturmfels, *Introduction to Chow forms*, in Invariant methods in discrete and computational geometry (N. White, ed.), Springer, New York, 1995, pp. 37–58.
10. M. Démazure, *Sur deux problèmes de reconstruction*, Technical Report **882**, INRIA, Rocquencourt, 1988.
11. S. Di Rocco, *Linear toric fibrations*, in Combinatorial algebraic geometry, Lecture Notes in Mathematics **2108**, Springer, Cham, 2014, pp. 119–147.
12. D. Eisenbud and J. Harris, *On varieties of minimal degree (a centennial account)*, in Algebraic geometry, Bowdoin 1985, Part 1, Proceedings of Symposia in Pure Mathematics **46** (S.J. Bloch, ed.), American Mathematical Society, Providence, 1987, pp. 3–13.
13. J.-C. Faugère, *A new efficient algorithm for computing Gröbner bases (F4)*, *J. Pure Appl. Algebra* **139** (1999) 61–88.
14. M. Fischler and R. Bolles, *Random sample consensus: a paradigm for model fitting with applications to image analysis and automated cartography*, *Commun. ACM* **24** (1981) 381–395.
15. A. Fitzgibbon, *Simultaneous linear estimation of multiple view geometry and lens distortion*, in Proceedings of the 2001 IEEE Conference on Computer Vision and Pattern Recognition (CVPR 2001), pp. 125–132.
16. G. Fløystad, J. Kileel and G. Ottaviani, *The Chow form of the essential variety in computer vision*, *J. Symbolic Comput.*, to appear.
17. I.M. Gel'fand, M.M. Kapranov and A.V. Zelevinsky, *Discriminants, resultants and multidimensional determinants*, Birkhäuser, Boston, 1994.
18. D. Grayson and M. Stillman, *Macaulay2, a software system for research in algebraic geometry*, available at [www.math.uiuc.edu/Macaulay2/](http://www.math.uiuc.edu/Macaulay2/).
19. J. Harris, *Algebraic geometry: a first course*, Graduate Texts in Mathematics **133**, Springer-Verlag, New York, 1992.
20. R. Hartley and A. Zisserman, *Multiple view geometry in computer vision*, Cambridge University Press, 2nd ed., Cambridge, 2003.
21. A. Jensen, *Gfan, a software system for Gröbner fans and tropical varieties*, Available at <http://home.imf.au.dk/jensen/software/gfan/gfan.html>.
22. F. Jiang, Y. Kuang, J.E. Solem and K. Åström, *A minimal solution to relative pose with unknown focal length and radial distortion*, in Proceedings of the 2014 Asian Conference on Computer Vision (ACCV 2014), pp. 443–456.
23. M. Kapranov, B. Sturmfels and A. Zelevinski, *Chow polytopes and general resultants*, *Duke Math. J.* **67** (1992) 189–218.
24. Y. Kuang, J.E. Solem, F. Kahl and K. Åström, *Minimal solvers for relative pose with a single unknown radial distortion*, in Proceedings of 2014 IEEE Conference on Computer Vision and Pattern Recognition (CVPR 2014), pp. 33–40.
25. Z. Kukeleva, *Algebraic Methods in Computer Vision*, Doctoral Thesis, Czech Technical University in Prague, 2013.
26. Z. Kukeleva, M. Bujnak and T. Pajdla, *Automatic Generator of Minimal Problem Solvers*, in Proceedings of the 2008 European Conference on Computer Vision (ECCV 2008), Lecture Notes in Computer Science **5304**, Springer 2008, pp. 302–315.
27. D. Maclagan and B. Sturmfels, *Introduction to Tropical Geometry*, Graduate Studies in Mathematics **161**, American Mathematical Society, 2015.
28. B. Micusik and T. Pajdla, *Structure from motion with wide circular field of view cameras*, *IEEE T. Pattern Anal.* **28** (2006) 1135–1149.
29. G. Newsam, D. Q. Huynh, M. Brooks and H. P. Pan, *Recovering unknown focal lengths in self-calibration: an essentially linear algorithm and degenerate configurations*, *ISPRS J. Photogramm.*, vol. XXXI-B3 (1996), 575–580.



30. D. Nistér, *An efficient solution to the five-point relative pose problem*, IEEE T. Pattern Anal. **26** (2004) 756–770.
31. S. Petrović, *On the universal Gröbner bases of varieties of minimal degree*, Math. Res. Lett. **15** (2008) 1211–1221.
32. H. Stewenius, D. Nistér, F. Kahl and F. Schaffalitzky, *A minimal solution for relative pose with unknown focal length*, in Proceedings of the 2005 IEEE Computer Society Conference on Computer Vision and Pattern Recognition (CVPR 2005), pp. 789–794.
33. P. Sturm, *On focal length calibration from two views*, in Proceedings of the 2001 IEEE Conference on Computer Vision and Pattern Recognition (CVPR 2001), pp. 145–150.
34. B. Sturmfels, *Gröbner bases and convex polytopes*, American Mathematical Society, University Lectures Series **8**, Providence, 1996.
35. B. Sturmfels, *Solving systems of polynomial equations*, American Mathematical Society, CBMS Regional Conferences Series **97**, Providence, 2002.
36. C. Traverso, *Gröbner trace algorithms*, in Proceedings of the 1988 International Symposium of Symbolic and Algebraic Computation (ISSAC 1988), Lecture Notes in Computer Science **358** (P. Gianni, ed.), Springer-Verlag, Berlin Heidelberg, 1989, pp. 125–138.